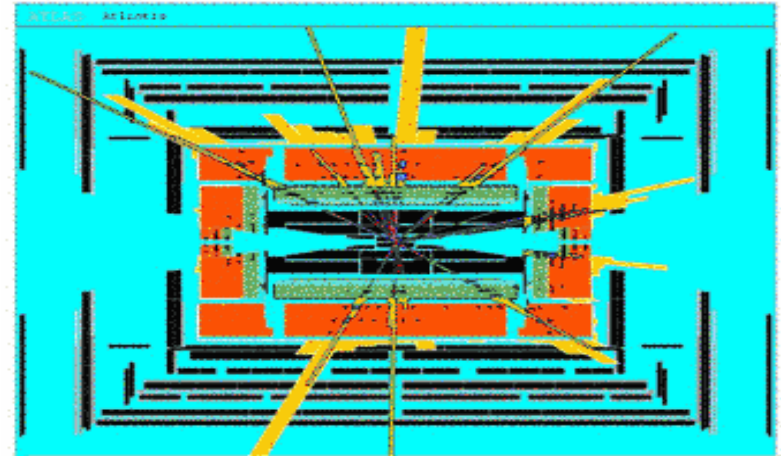


TeV-Scale BLACK HOLES @ the LHC

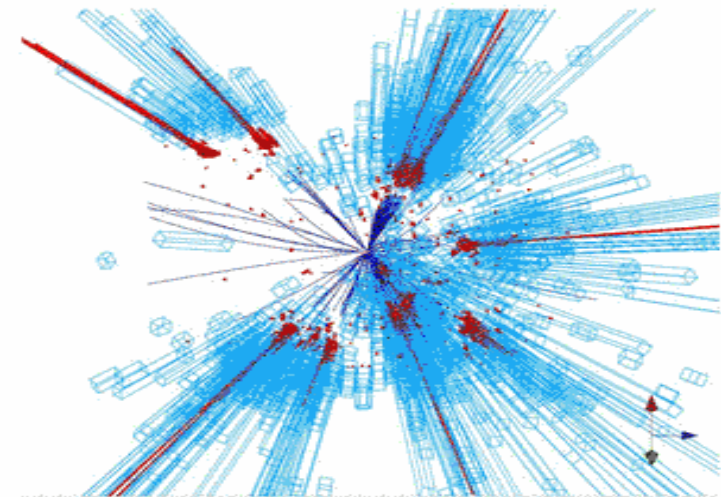


©Original Artist
Reproduction rights obtainable from
www.CartoonStock.com

Professor Landsberg was fast regretting becoming the first man to successfully create a mini black hole in the laboratory.



Simulation of a Quantum Black Hole event



Simulation of a black hole event with $M_{BH} \sim 8$ TeV in CMS



Cartoons and Tom Hanks aside, I will not talk about LHC Death-by-BH scenarios ! These are excluded by astrophysics & the general arguments by Giddings & Mangano given in arXiv:0806.3381 & 0808.4087.

After all...we're still here!!

- TeV-scale BH are usually discussed within the context of ED models involving gravity with $D=n+4$, e.g., ADD and/or RS.
- For all practical purposes the BH in RS=ADD($n=1$) *provided* the BH horizon radius, r_h and the RS AdS curvature, k , satisfy

$$(kr_h)^2 \ll 1 \quad ds^2 = e^{-2k|y|} \eta_{\mu\nu} dx^\mu dx^\nu - dy^2 ,$$

which we can check a posteriori, *if* the SM fields are restricted to the TeV brane. Bulk SM fields are more complicated..

- In all cases it is assumed that the BH does not globally modify the model's setup/metric and that the ADD/RS compactification radius is large compared to r_h so that the BH does not 'see' the spatial curvature in the higher dimensions: $(r_h / R_c)^2 \ll 1$ which can also be checked a posteriori.

Notational Issues

WARNING!!!

$$S = \int d^{4+n}x \sqrt{-g} \frac{M_*^{n+2}}{2} \left[R + \frac{\alpha}{M_*^2} \mathcal{L}_2 + \frac{\beta}{M_*^4} \mathcal{L}_3 + \frac{\gamma}{M_*^6} \mathcal{L}_4 \right]$$

$$S_{int} = \int d^4x d^n y \frac{-1}{M_*^{1+n/2}} \sum_n h_{\mu\nu}^{(n)} T^{\mu\nu} \delta(y)$$

Graviton-SM matter interaction

→ $\overline{M}_{Pl}^2 = V_n M_*^{n+2}; \quad V_n = (2\pi R_c)^n$

For toroidal compactifications

Note that M_* can be related to several other mass parameters used in the literature. The Planck scale employed by Dimopoulos and Landsberg[8] is given by $M_{DL} = (8\pi)^{1/(n+2)} M_*$ while that of Giddings and Thomas[9] is found to be $M_{GT} = [2(2\pi)^n]^{1/(n+2)} M_*$; moreover, Giudice *et al.*[3] employ a different scale $M_D = (2\pi)^{n/(n+2)} M_*$. Further note that M_* is thus correspondingly smaller than all of these other parameters with consequently far weaker bounds[2]. For example, if $n = 2(6)$ and $M_D = 1.5$ TeV then $M_* = 0.60(0.38)$ TeV; 4

BH Formation in High Energy Collisions

- **Thorne's Hoop Conjecture:** A D-dimensional horizon, i.e., a BH, forms when M (or E) is compressed into a region whose 'area in all directions' satisfies $A_{D-3} < G_D M$. This has **not been proven** in all generality but seems to be verified in numerical analyses & simulations.

Simplest Case: Head on collision, no angular momentum, no gravitational energy loss, no..... The cross section is then

Full collision energy forms BH

$$\hat{\sigma} = \pi R_s^2 (n, M_{\text{BH}} = \sqrt{\hat{s}}) \theta(\sqrt{\hat{s}} - M_*)$$

D=n+4 Schwarzschild radius

A threshold at the Planck scale where gravity becomes strong is *assumed*

Banks & Fischler
Giddings & Thomas
Dimopoulos & Landsberg

$$\underline{R_s = ??}$$

$$\longrightarrow M_{BH} / M_* = c (M_* R_s)^{n+1} \quad c = \frac{(n+2)\pi^{(n+3)/2}}{\Gamma(\frac{n+3}{2})}$$

so at a collider....

All possible
parton pairs

$$\frac{d\sigma_{pp \rightarrow BH+X}}{dM}(s) = \frac{2M}{s} \sum_{a,b} \int_{M^2/s}^1 \frac{dx}{x} f_a\left(\frac{\tau}{x}\right) f_b(x) \hat{\sigma}_{ab \rightarrow BH}(\hat{s} = M^2)$$

$$\sigma = \int_{M_{BH}^{min}{}^2/s}^1 d\tau \int_{\tau}^1 \frac{dx}{x} \sum_{ab} f_a(x) f_b(\tau/x) \hat{\sigma}(M_{BH})$$

$$M_{BH}^{min} = x_{min} M_*$$

$$Q \text{ (pdf 's)} = M_{BH}, 1/R_s \text{ ???}$$

One may argue that the **threshold region** is quantum dominated so GR should not apply there & so $x_{min} = \text{'several' (???)}$

Warning (Again!)

$R_s (M_* = 1 \text{ TeV})$

$R_s (M_D = 1 \text{ TeV})$

$R_s (M_{GT} = 1 \text{ TeV})$

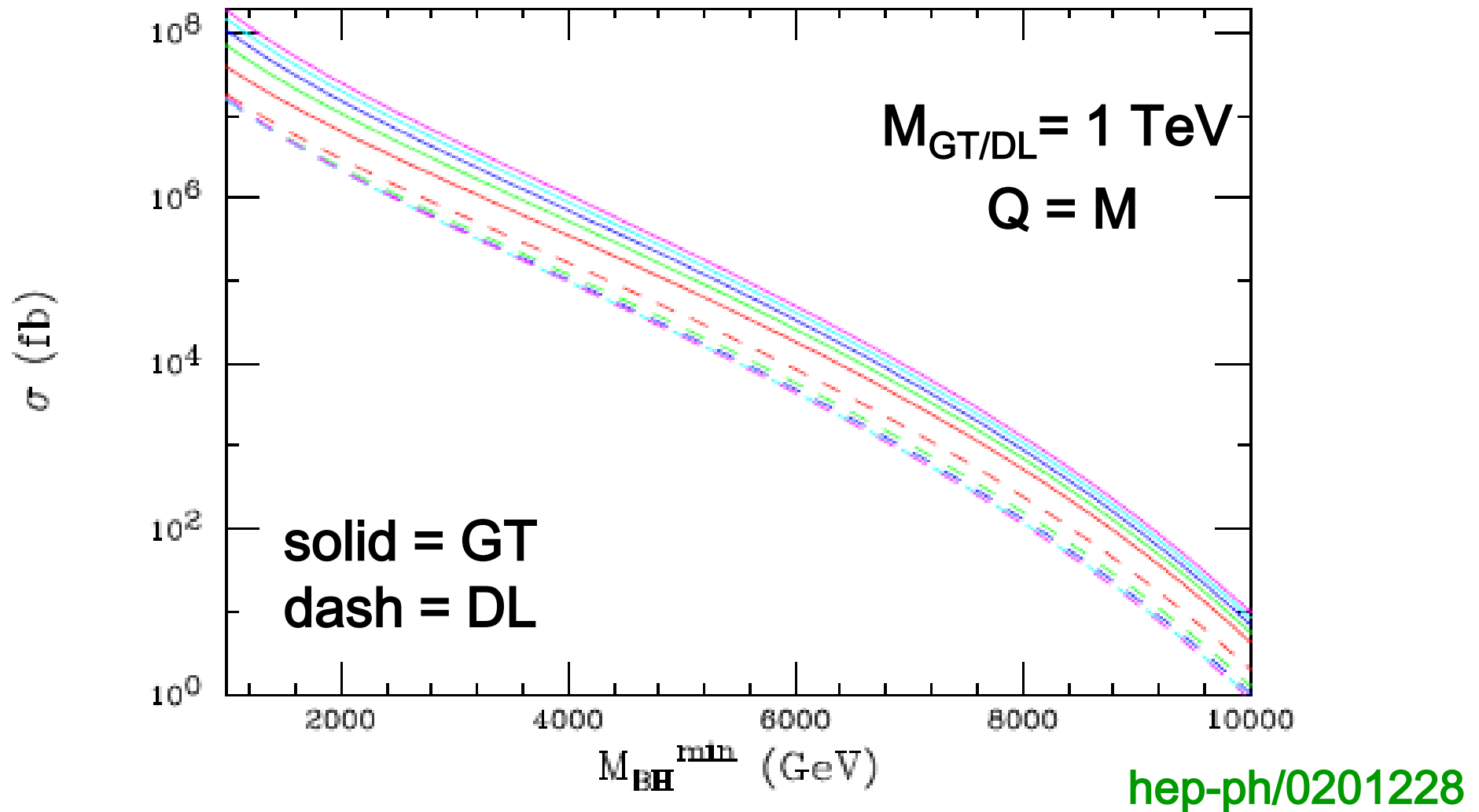
$R_s (M_{DL} = 1 \text{ TeV})$

These are all
different !!!
when all other
parameters are
fixed

...which can be easily seen on the cross section plot..
Even the n-dependence of the cross section can be
different !

Be careful when reading & using the literature....

But no matter what these are **HUGE** cross sections...



...hundreds of events even at very low luminosity !!!

This got people interested in this subject back in 2001...

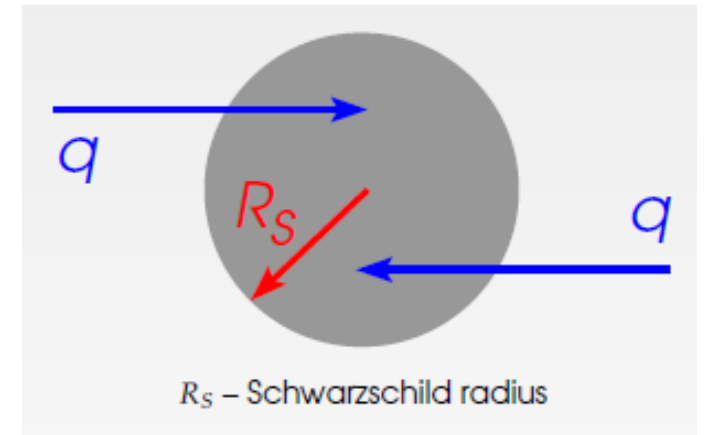
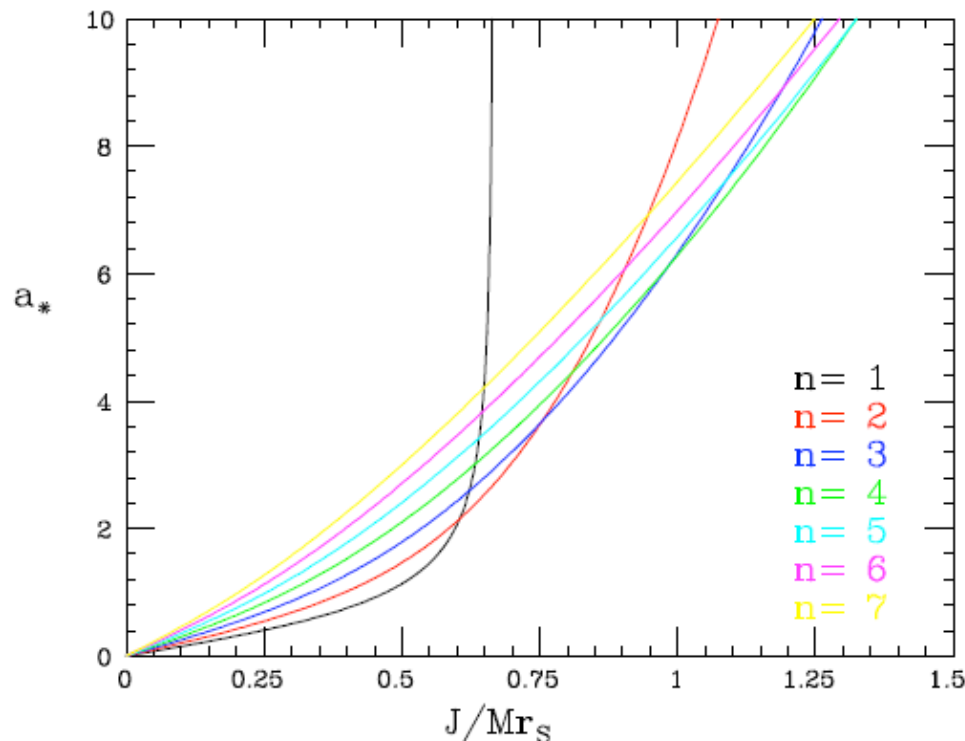
v.2 Myers-Perry D-dimensional Rotating BH

We need to correct for **finite** impact parameters and for finite (single component) angular momentum of the BH : $b_{\max} = 2 r_h$

$$\hat{\sigma} = \textcircled{F} \pi R_s^2 (n, M = \sqrt{s}) \theta(\sqrt{s} - M_*)$$

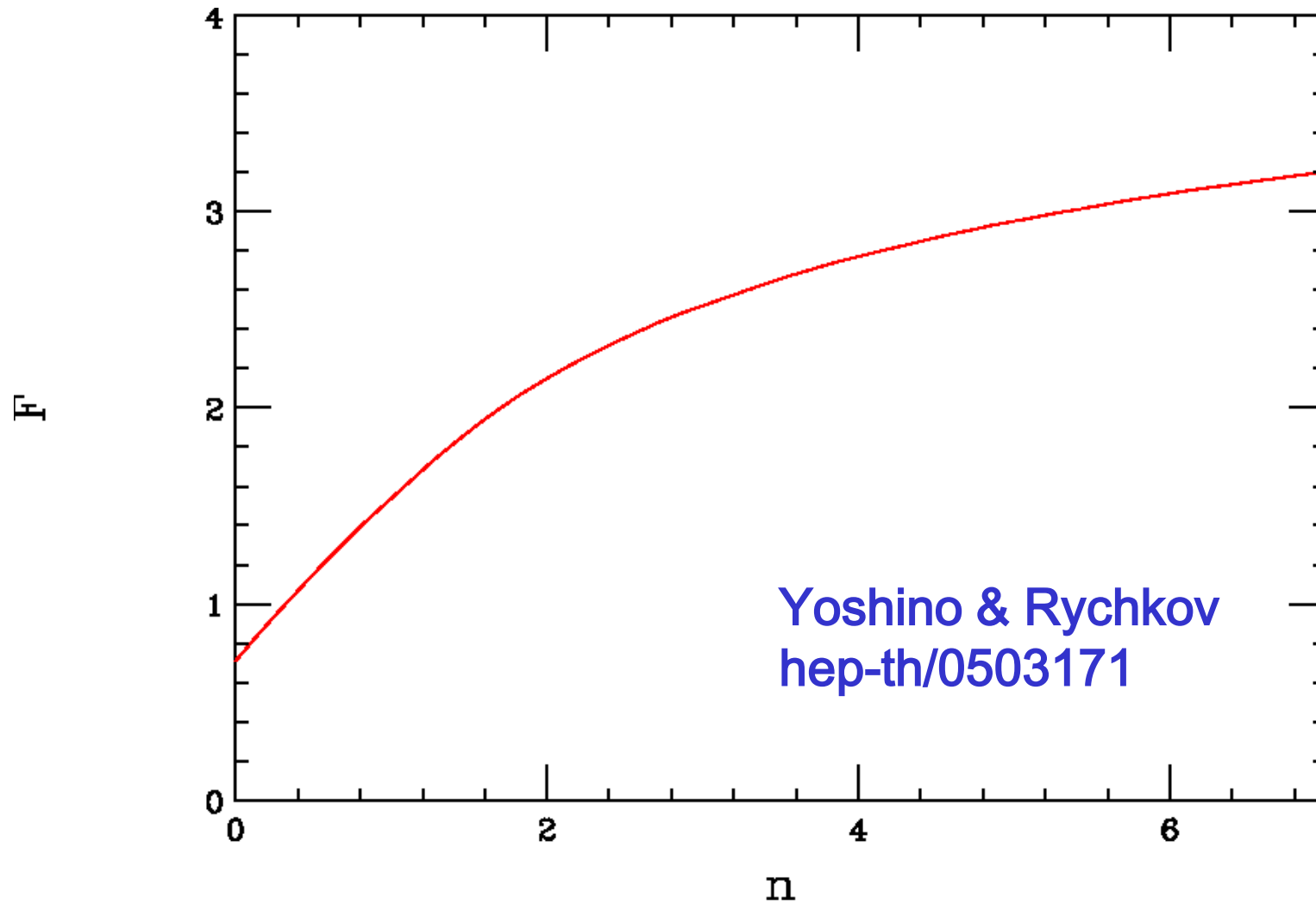
$$r_h = r_S \left(1 + a_*^2\right)^{-\frac{1}{n+1}}$$

$$a_* = \frac{(n+2)J}{2Mr_h}$$



J is the angular momentum
 r_h is the inner horizon radius

$F = ?? \rightarrow$ It's slightly larger than unity !



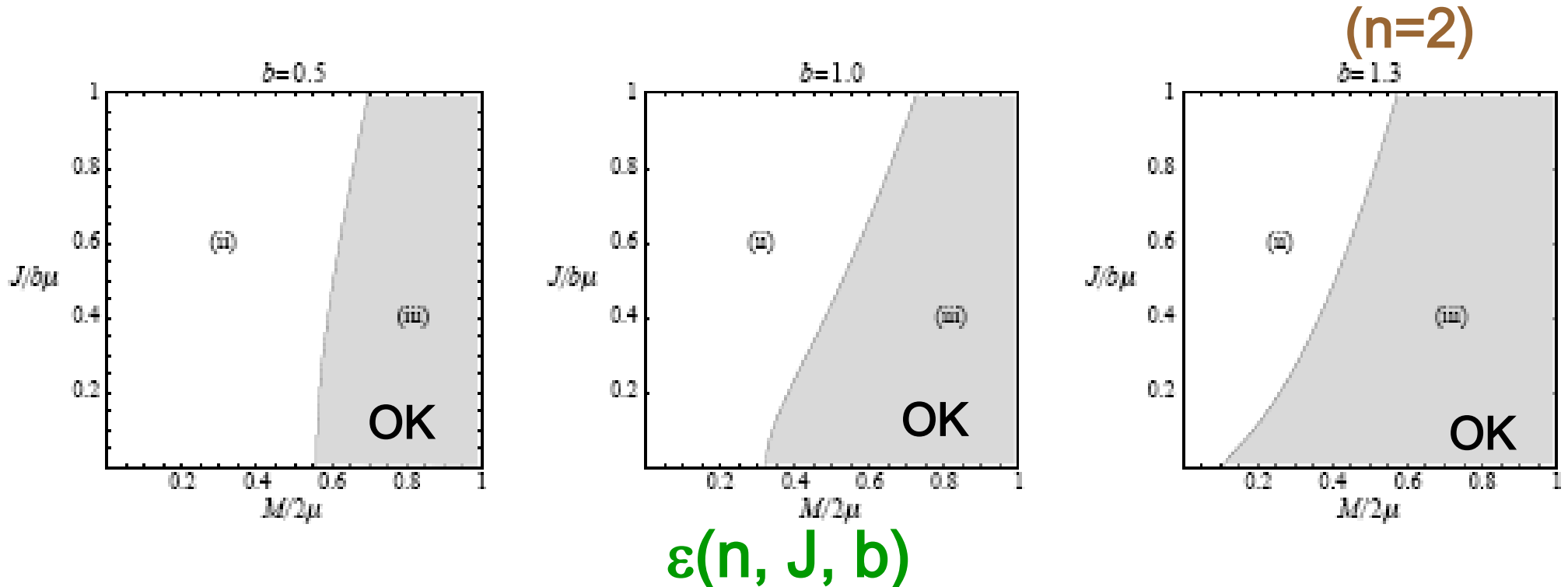
Obtained from the numerical study of the collision of 2 boosted Myers-Perry (Kerr) solutions. The cross section is **enhanced** at the v.2 level...

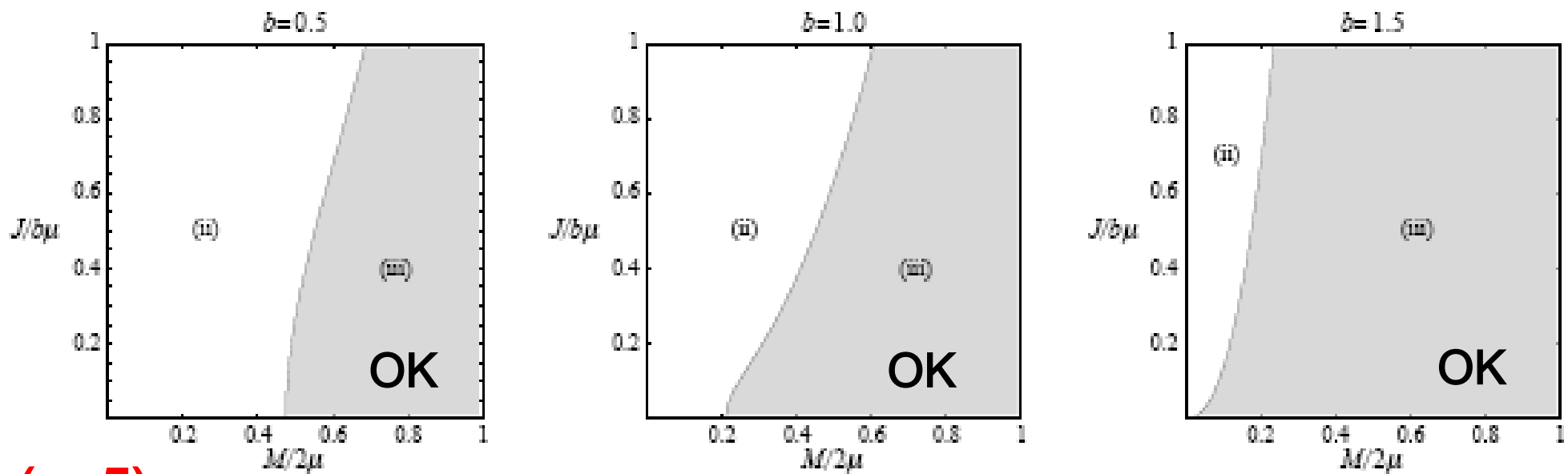
v.3

Not **all** of the center of mass energy in the partonic collision goes into BH formation due to lost gravitational radiation...

$$M = \varepsilon(n, J, b) \sqrt{\hat{s}}$$

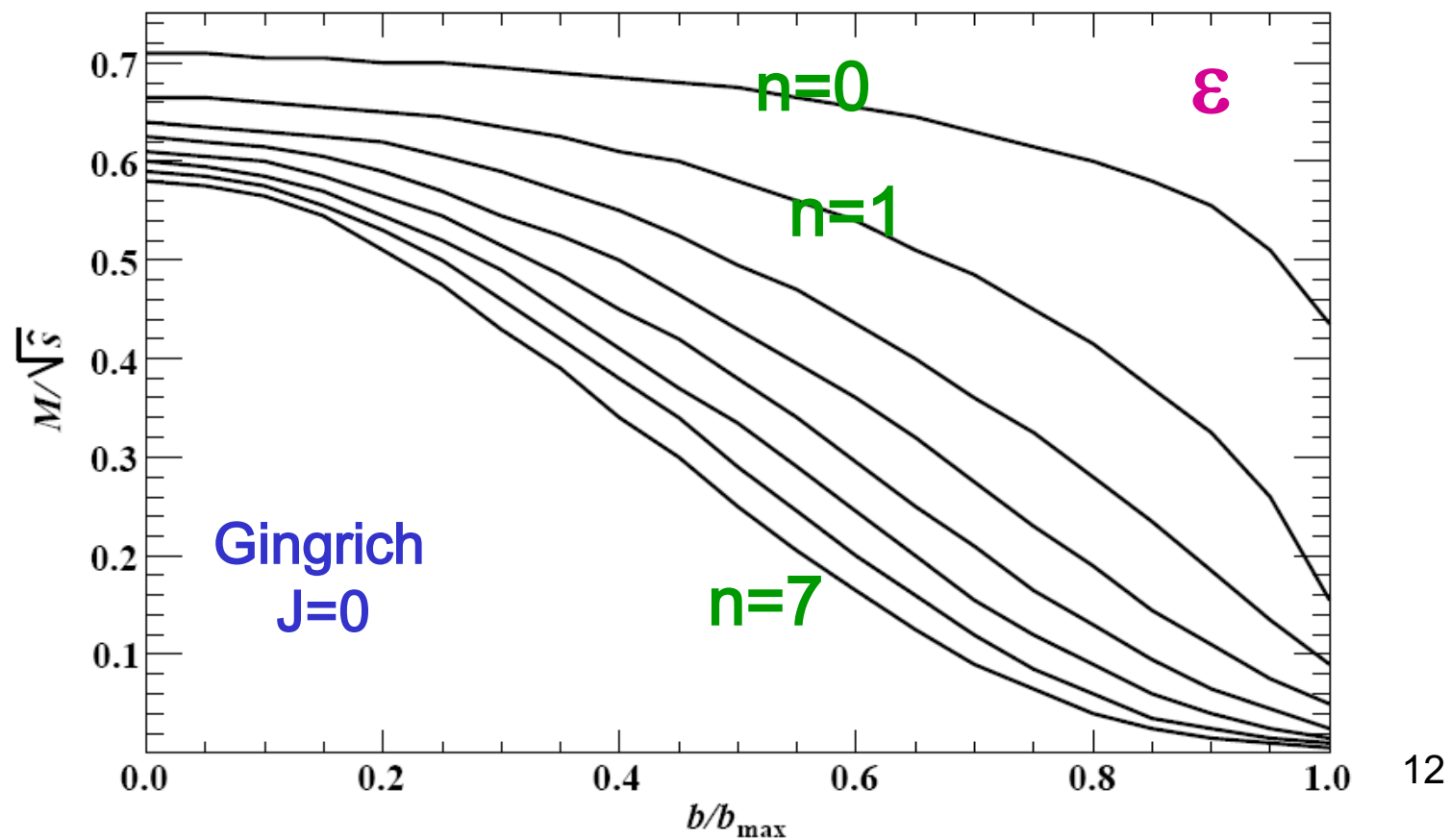
The 'efficiency', $\varepsilon(n, J, b)$, must be obtained from numerical calculations...but Yoshino & Rychkov only provide *lower limits on ε* :



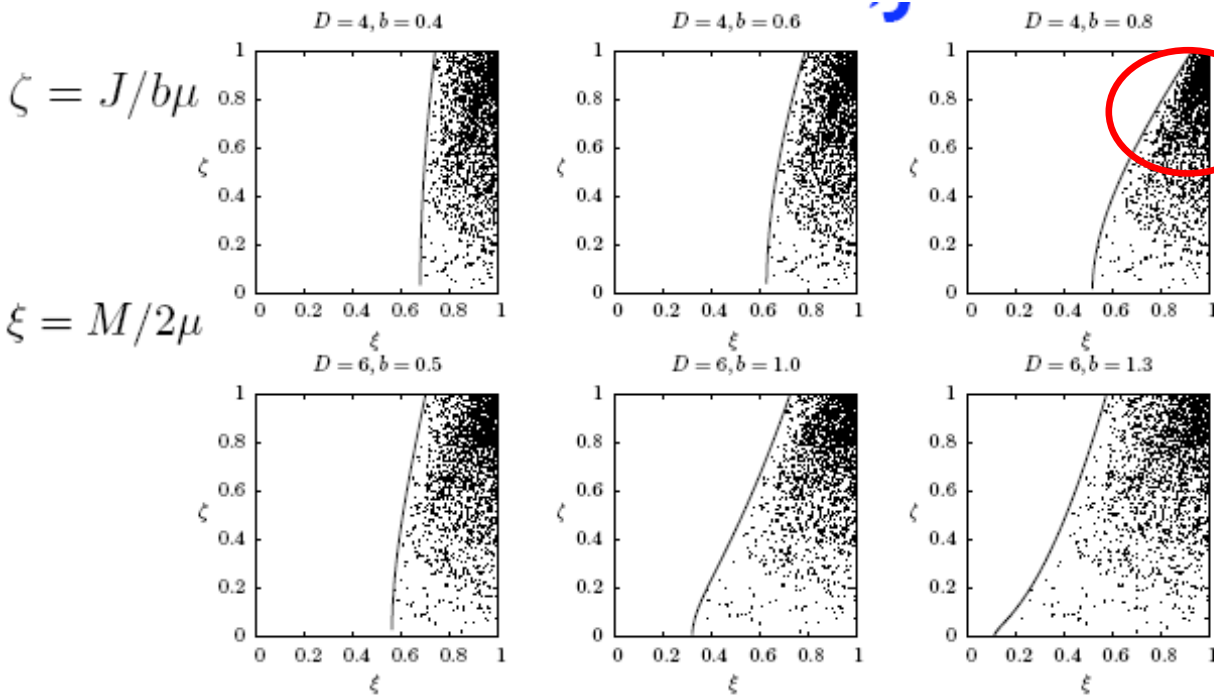


(n=5)

Similarly...



But what do we do in general? Construct a model...



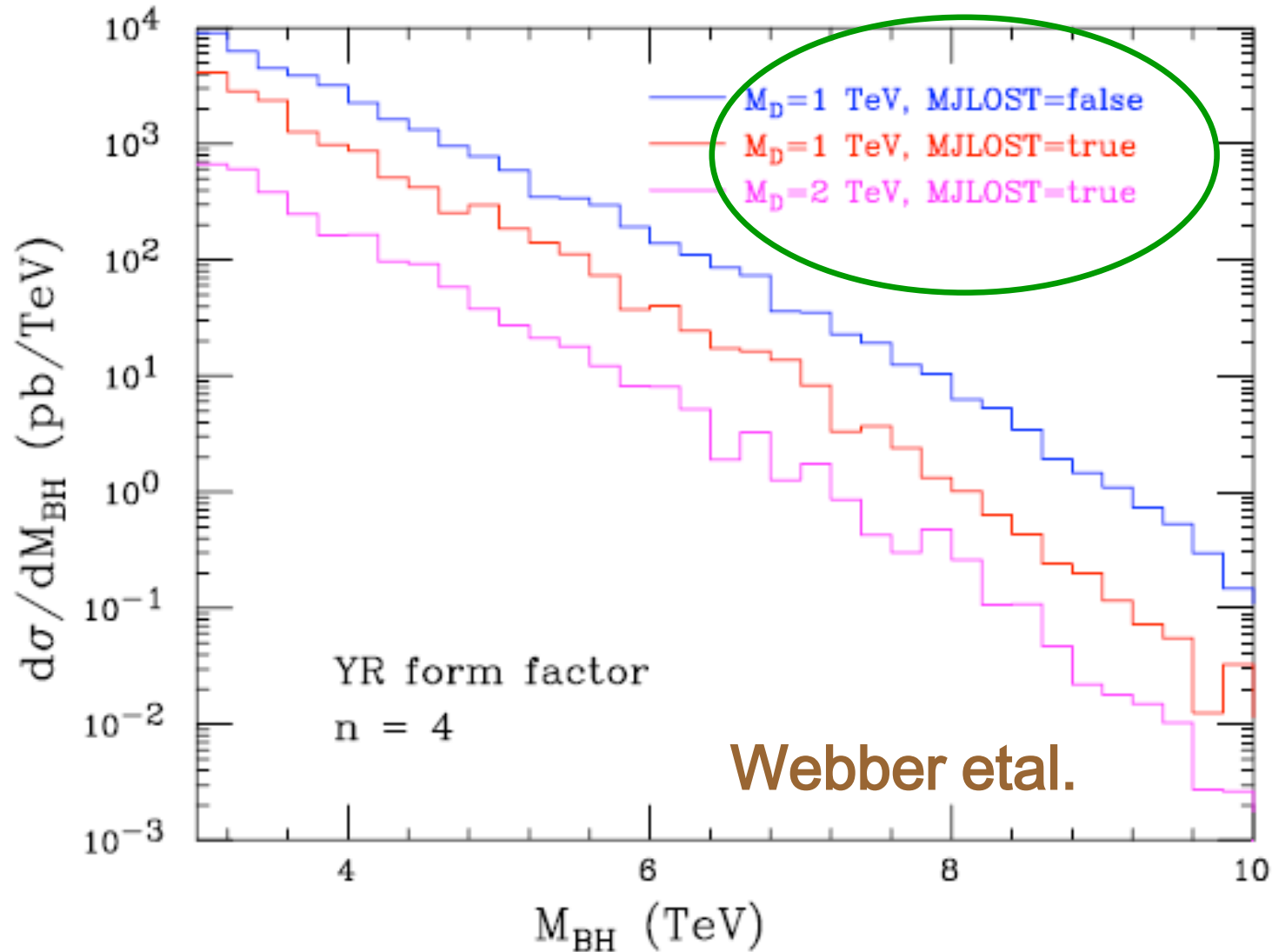
..here a 'linear' turn-on at the boundary is assumed. See Webber et al. for model details..

Most of the energy is trapped in BHs.. but it's just a model though it agrees with many other estimates when $b=0$

- Distribution vanishes on boundary curve
- Concentrated around $\Omega(M, J) = \Omega(2\mu, b\mu)$

These effects, though significant, still lead to large rates for BH production at the LHC...

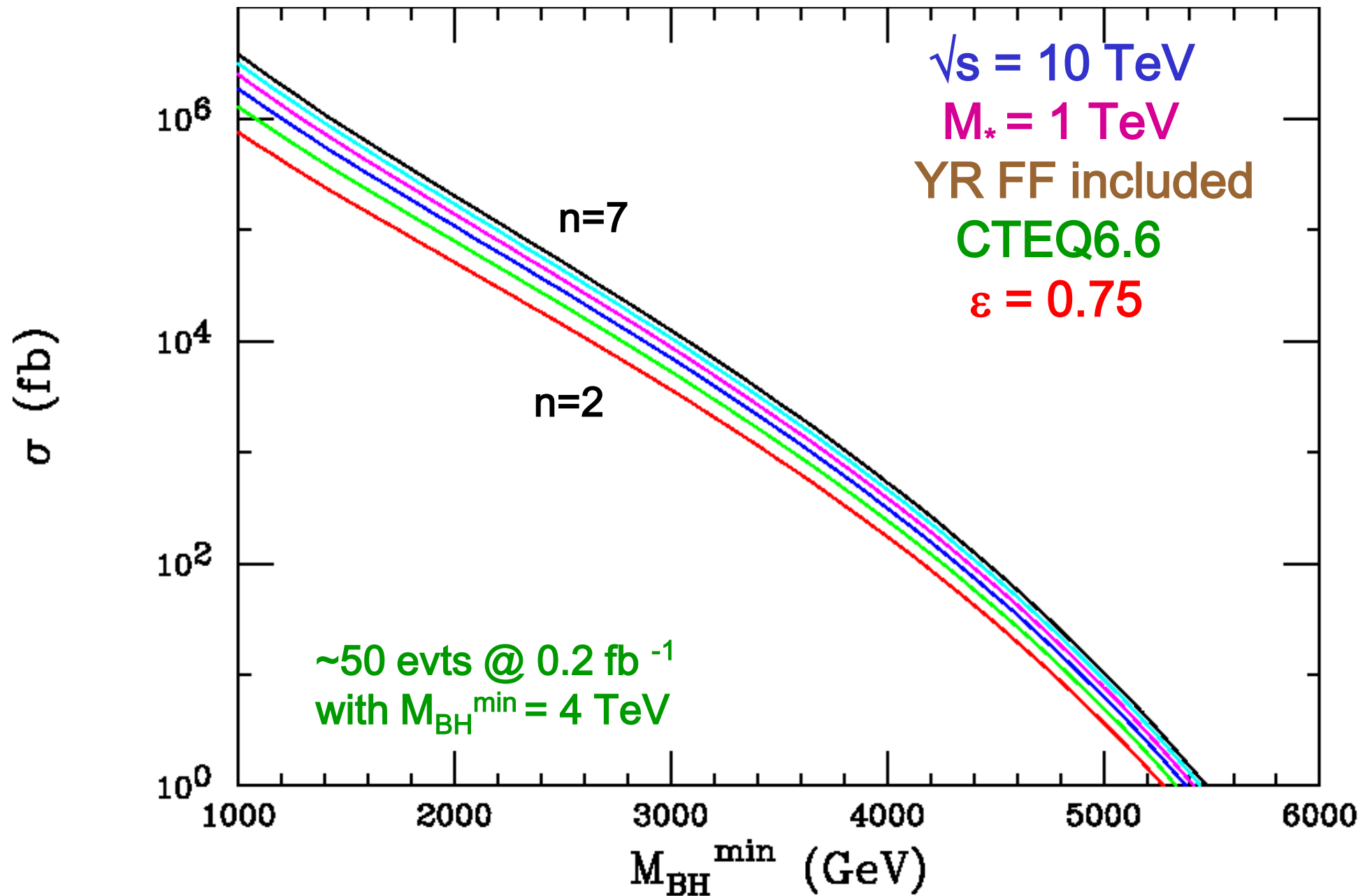
Large BH cross section at LHC



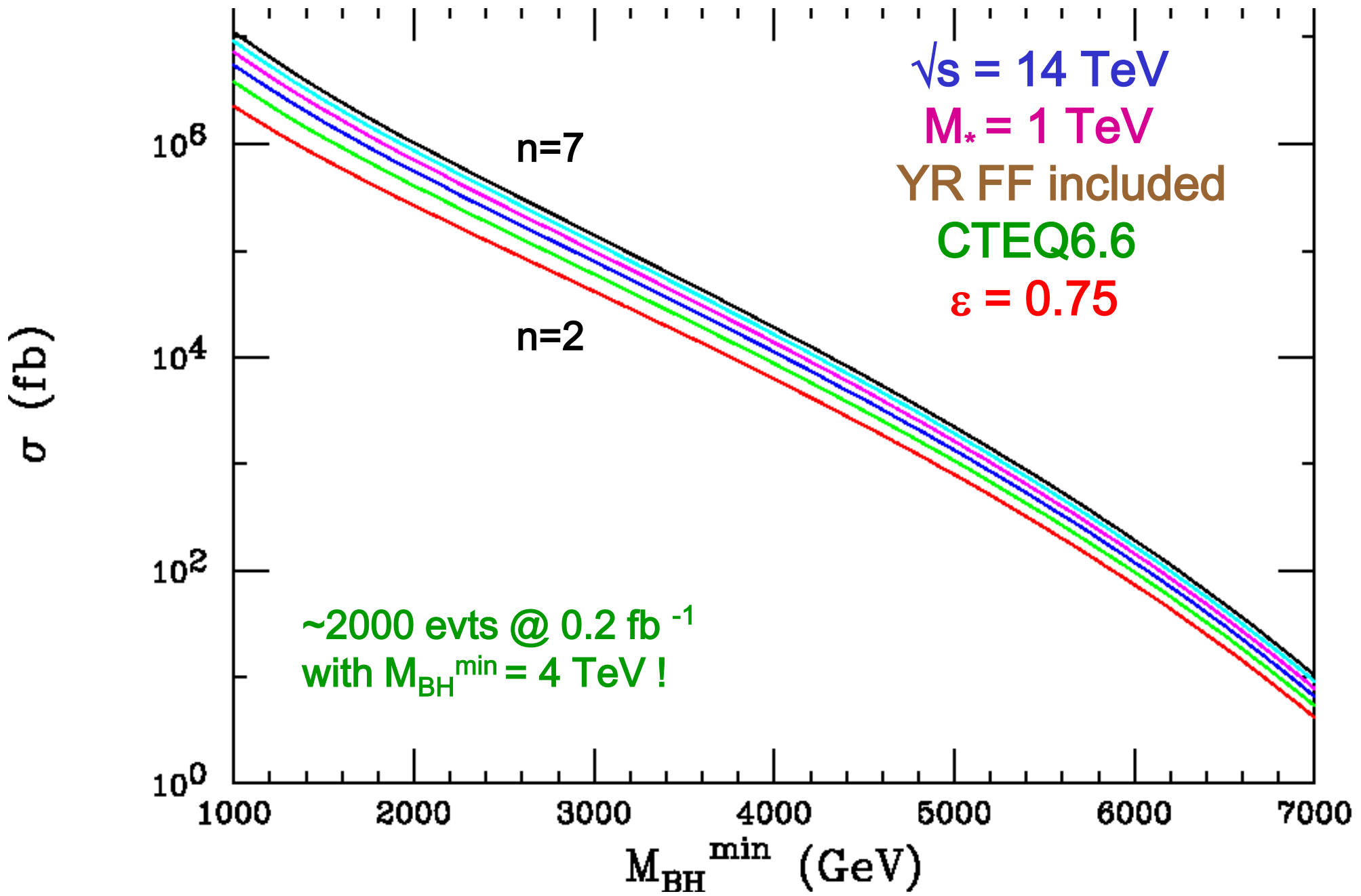
➔ A ~ 5 TeV BH per minute at LHC!

Charybdis2.0 (0904.0979, just released on the market)

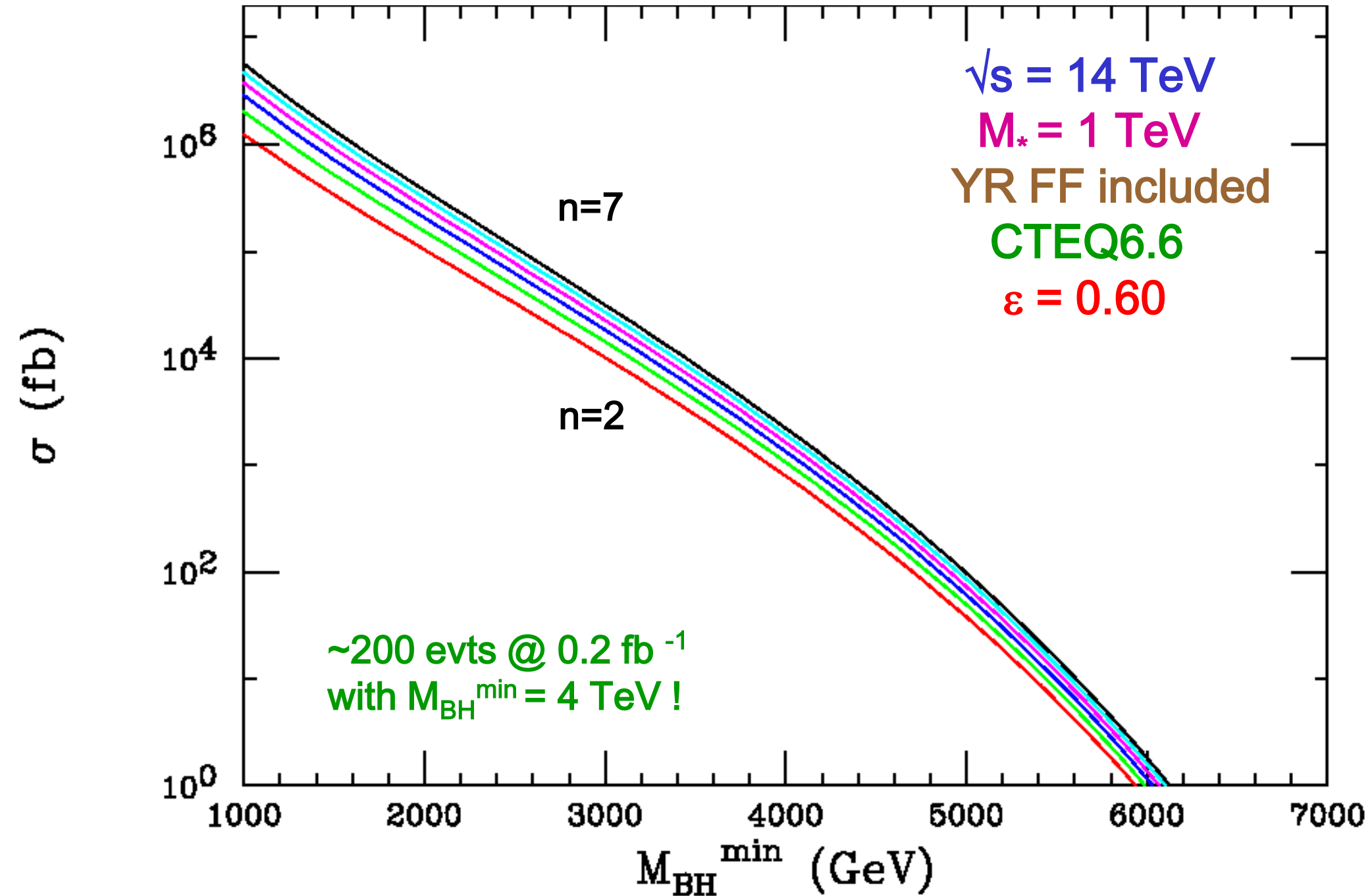
Updated Total Cross Section



...but the rates are much *larger* at 14 TeV...



...but knowing the efficiency is **critical**



v.4 Charge Effects ?

Yoshino & Mann
Gingrich

At the LHC, most of the colliding partons carry **EM charges** and all carry non-abelian **color** charges...is this important in the formation process? Can a '**Coulomb barrier**' prevent BH from forming? Even the EM case has not yet been explored in any model-independent way.

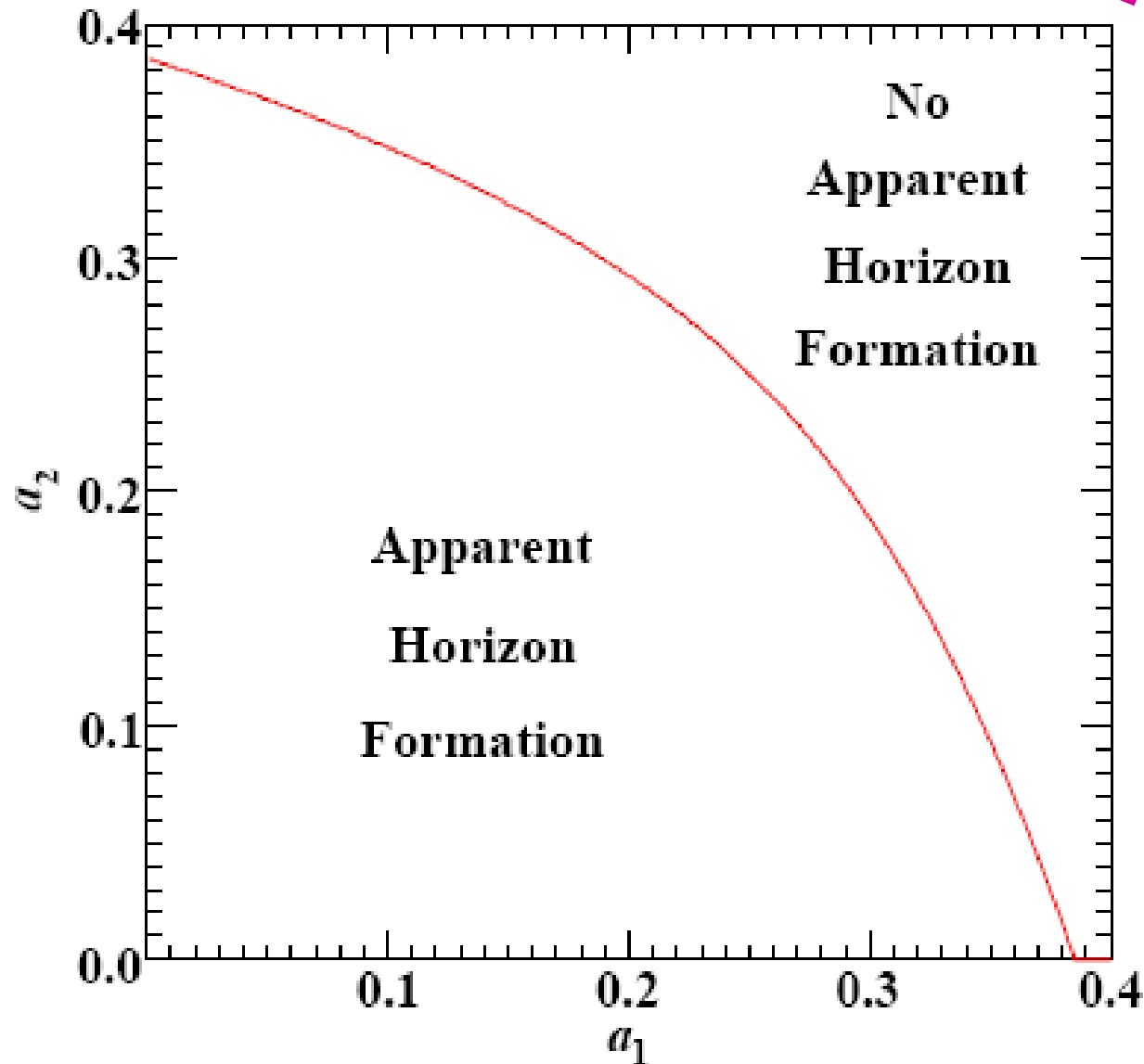
For EM, authors use **boosted collisions of Reissner-Nordstrom BH** (without angular momentum) & have the EM fields extending throughout a thick brane **assuming** the horizon radius is **smaller** than the brane thickness so that the D-dimensional solution is **applicable**. This is certainly a **very** questionable assumption.

Solutions with only 4-d EM fields are not yet known & further exploration is more than warranted.

$$a = \frac{2\pi(4\pi G_D p_e^2)}{D-3} \frac{(2D-5)!!}{(2D-4)!!}$$

$$p_e^2 = \gamma q^2$$

$$q^2 = q_4^2 \left(\frac{C_{\text{brane}}}{M_D} \right)^{D-4}$$



boost

Brane thickness

Gingrich

Comments :

- **Some experts believe** that this approach is not applicable as the EM fields extend into the **extra dimensions** although the SM is supposed to be 4-D. Putting in a thick brane allows extension of the EM field to D-dimensions but the geometry is not really multi-D spherically symmetric in any **physically realizable limit** since it requires the horizon radii to be much smaller than the brane thickness. Until the proper background metric can be employed where the EM fields are properly treated only in 4-D & explored, the **jury is still out** as to whether or not these **'EM'** effects are important.

v.5 Bulk SM Fields ????

In modern RS models the SM fields are in the bulk so the overlap of their 5-d wavefunctions is **important** in determining the BH cross section. ADD (n=1) + $(kR_S)^2 \ll 1$ + simple scaling leads to

$$(\sigma_{BH})_{12} = \int_{-\pi r_c}^{\pi r_c} dy \hat{\sigma}_{BH}(y) f_1(y) f_2(y) \quad \hat{\sigma}_{BH}(y) = \epsilon^2 \frac{M_{BH}|_{TeV}}{3\pi M_*^3} e^{2ky} = \sigma_0 e^{2k(y-\pi r_c)}$$

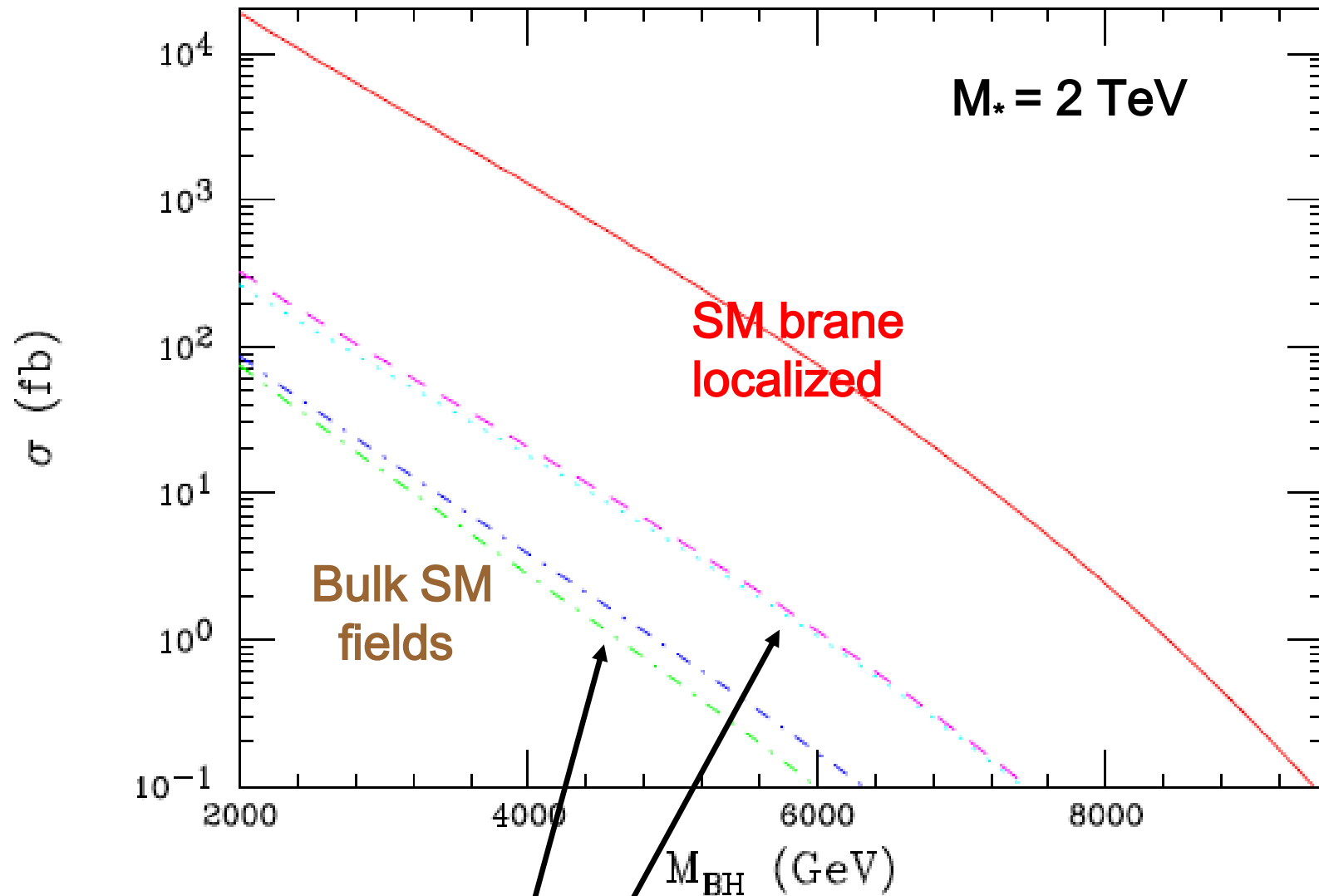
E.g.,

$$\sigma_{BH,gg} = S_{gg} \sigma_0 = \frac{\sigma_0}{2\pi k r_c} \simeq \frac{1}{71} \sigma_0 \quad !!$$

$$S_{gf} = \frac{1}{\sqrt{\pi k r_c}} \frac{\sqrt{1+2\nu}}{\nu+5/2} \frac{e^{\pi k r_c(\nu+1/2)} - \epsilon^2}{[e^{\pi k r_c(2\nu+1)} - 1]^{1/2}}$$

etc.

→ Substantial cross section reduction



Different fermion localizations

hep-ph/0611224

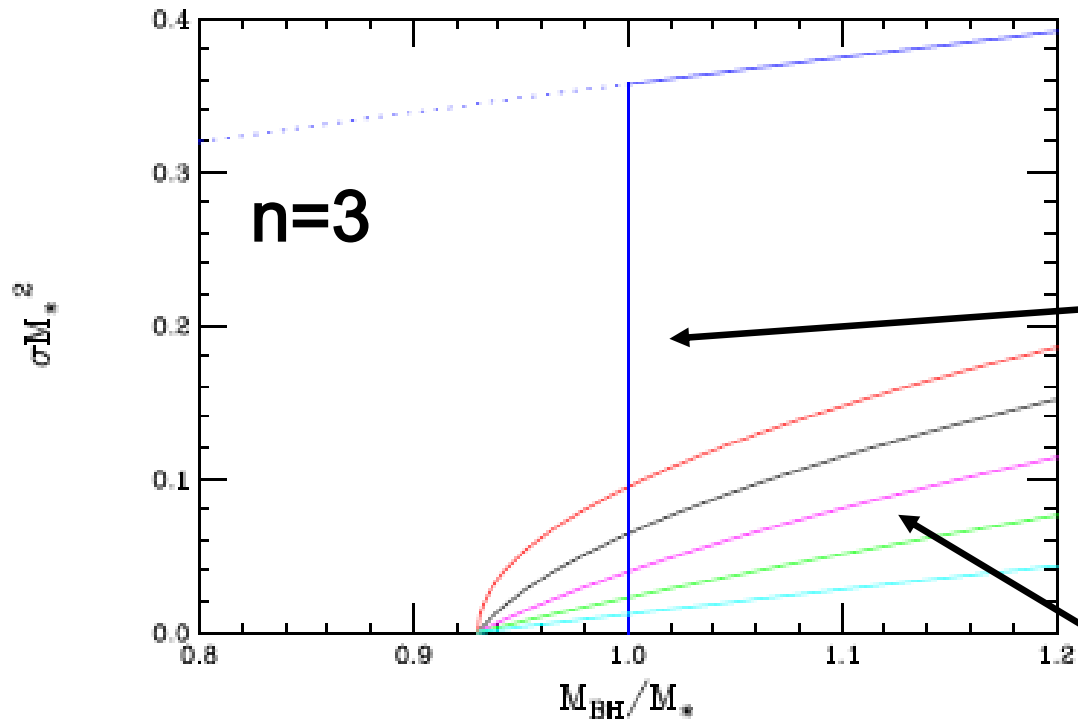
v.6

The threshold region is certainly **NOT** a step function but we can only speculate what goes on there w/o quantum gravity. Many models do predict a mass threshold due new 'QG'-like effects :

- Higher curvature terms [hep-ph/0503163](#)
- Non-commutative gravity [hep-ph/0606051](#)
- Gravitation fixed-points [hep-th/0511260](#)
- Resummed/RGE-improved gravity [hep-ph/0607198](#)
- Loop QG inspired [gr-qc/0503041](#)
- Minimum length [hep-ph/0305223](#)

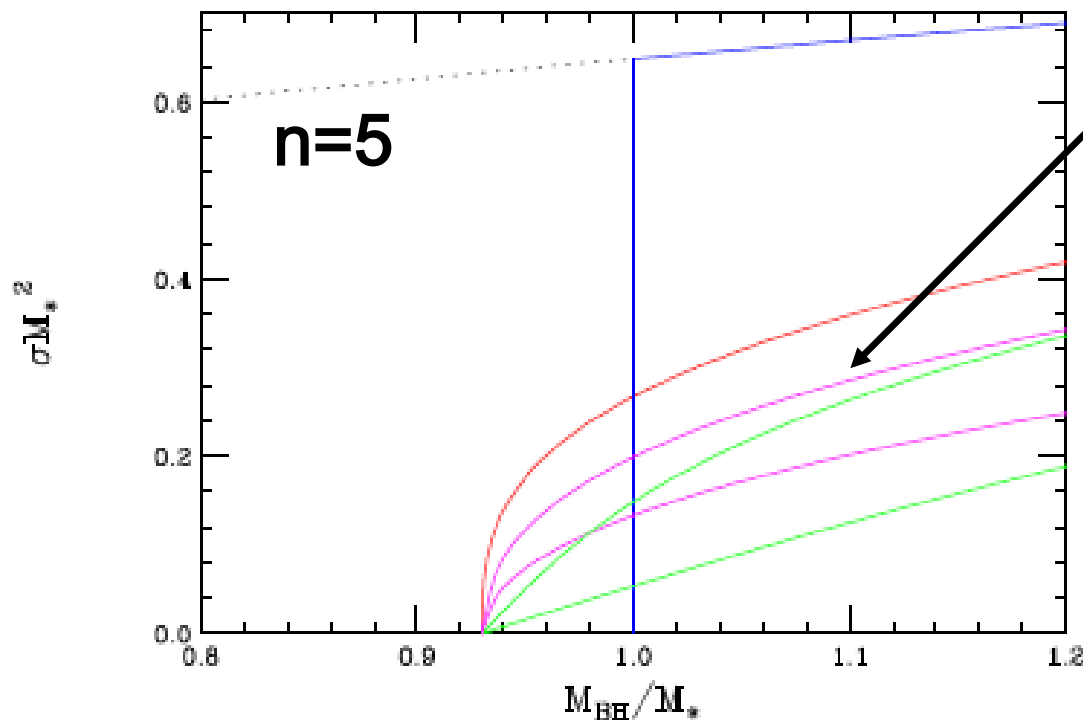
Or things may be *completely* different and String Balls are produced ! [hep-ph/0108060](#)

These assumptions also influence the final stages of BH decay.



For example:

'standard' step-function threshold for BH production



Thresholds induced by various higher curvature terms. These cross sections asymptote to the 'usual' results at large BH masses where the higher curvature terms become small.

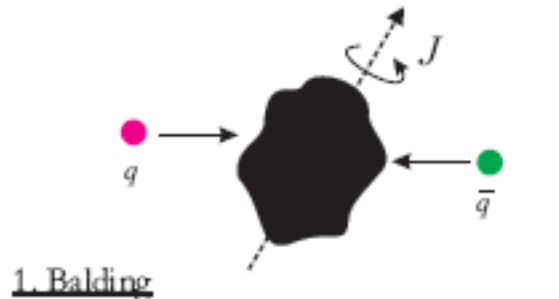
v.7

We need to include the effect of the spins of the colliding particles...this is still only at the beginning stages..

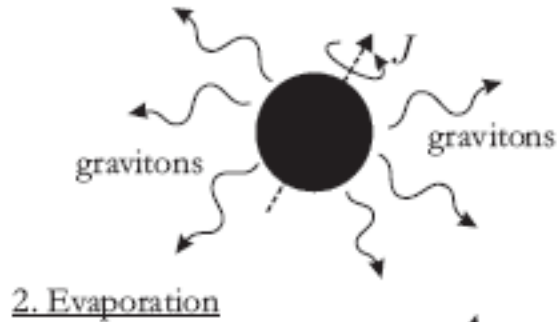
**Yoshino, Zelnikov
& Frolov**

BH Decay

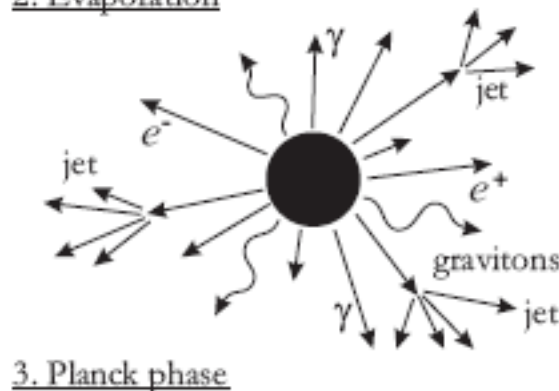
After BH formation the BH will decay emitting gravitons (bulk) and various SM particles (brane). Loosely...



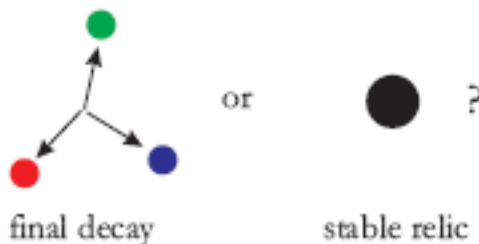
‘Balding’ Phase: loses ‘hair’ and multipole moments via gravitational radiation



Spin-down Phase: loses angular momentum and mass via Hawking radiation; becomes spherical



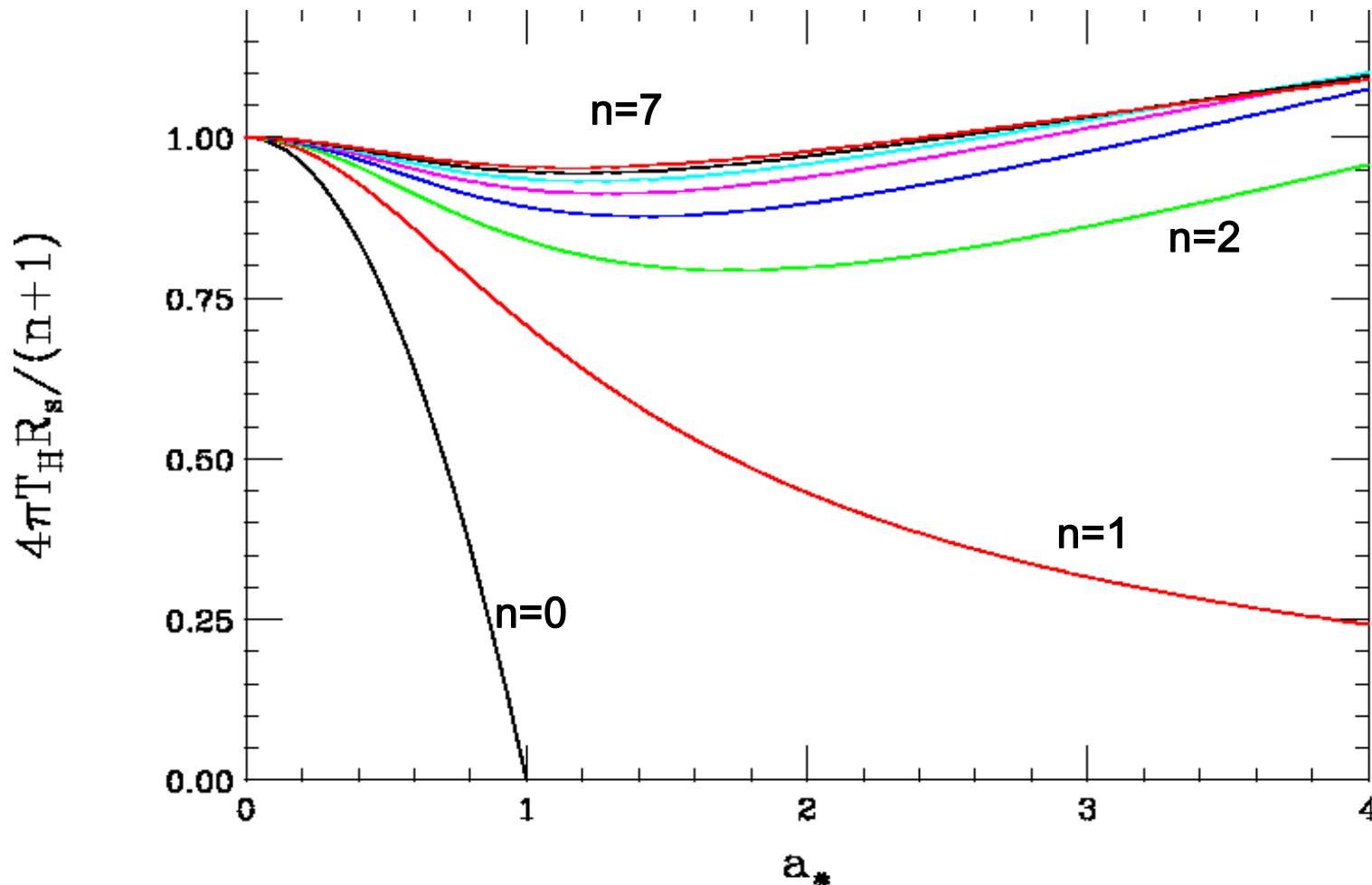
Schwarzschild Phase: loses mass by spherical emission of Hawking radiation while temperature increases (in GR)



Planck Phase: final decay **or** stable remnant determined by quantum gravity

Black hole decay is controlled by the **Hawking temperature** which is **not** very sensitive to rotation when $n > 1$:

$$T_H = \frac{(n+1)+(n-1)a_*^2}{4\pi r_h (1+a_*^2)} \quad \text{with} \quad a_* = \frac{(n+2)J}{2Mr_h}$$



Hawking radiation will consist of both the emission of SM fields on the brane (in ADD) as well as KK gravitons into the bulk.

For the simplest possible, non-rotating case (ignoring *all* details) one expects the mass loss by spherical emission of black-body SM radiation to be given by:

$$\frac{dM_{BH}}{dt} \sim R_S^2 \sum_i N_i \int_0^\infty d\omega \frac{\omega^3}{e^{\omega/T} + s_i} \sim R_S^2 T^4 \sum_i N_i Q_i$$

where $s_i = 1(-1)$ for fermions (bosons). This leads to *very* short BH lifetimes :

$$\tau \sim M_*^{-1} (M_{BH} / M_*)^{(n+3)/(n+1)} \sim 10^{-26} \text{ sec} \sim (100 \text{ GeV})^{-1}$$

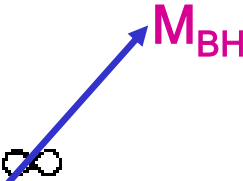
Of course, there are MANY corrections to this naïve estimate.

We have to correct this for lots of things including:

- (i) non-spherical emission from a rotating BH
- (ii) 'grey-body' factors that arise due to the equations of motion & associated BH 'barrier' boundary conditions for the emitted particles of various spins in the BH background
- (iii) the cooling of the BH as particles are emitted (canonical vs. microcanonical ensemble)
- (iv) account for graviton emission into the bulk
- (v) account for BH recoil during the emission process
- (vi) the possibility that a remnant may exist

Nobody has accounted for all of these possibilities simultaneously

The Grey-Body Factor is supposed to correct

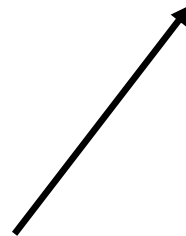
$$\int_0^\infty d\omega \frac{\omega^3}{e^{\omega/T} + s_i} \longrightarrow \sim \int_0^\infty d\omega \frac{\omega |A_{lm}^i(\omega, J)|^2}{e^{\omega/T} + s_i}$$


and contains both energy-dependent & angular emission info for a particular BH angular momentum and particle spin final state

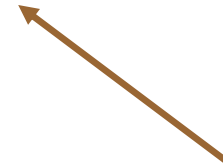
These are not easily obtained...

GBF, e.g., for a scalar field in the case of 4-d brane emission

$$\phi(t,r,\theta,\varphi) = \exp(-i\omega t) \exp(im\varphi) R(r) T_{lm}(\theta, J)$$



Satisfies radial KG equation in the Myers-Perry background



Spheroidal harmonics

R(horizon) must be in-falling plane waves in the rotating frame whereas R(∞) is a sum of in-going & out-going spherical waves:

$$R(\infty) = [A_{lm} \exp(i\omega r) + B_{lm} \exp(-i\omega r)] r^{-1}$$

The GB factors are then defined as the transmission coefficients $1 - K |A/B|^2$ for all (l,m) where K corrects for the particle spin ($K=1$ for scalars)

Needless to say, the GBF can only be obtained numerically especially for higher spins & decay into the bulk!

As of now, GBF have been calculated for spin=0, 1/2 & 1 for brane emission from a rotating BH as well as for bulk scalars. GBF for bulk graviton emission are, so far, known only in the Schwarzschild case.

Kanti etal
spin-0 brane
emission

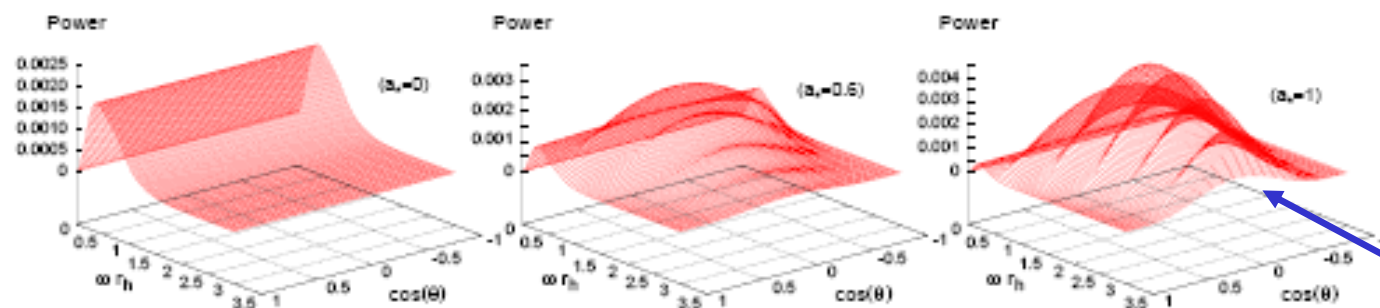


Figure 8: Angular distribution of the power spectra for scalar emission from rotating black holes, for $n = 1$ and $a_+ = (0, 0.6, 1)$.

Emission peaks
on the collision
plane as J is
increased

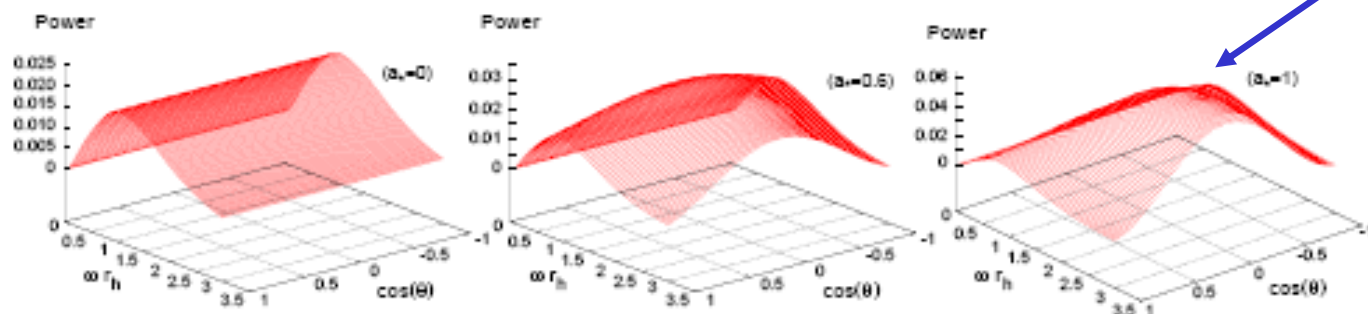


Figure 9: Angular distribution of the power spectra for scalar emission from rotating black holes, for $n = 4$ and $a_+ = (0, 0.6, 1)$.

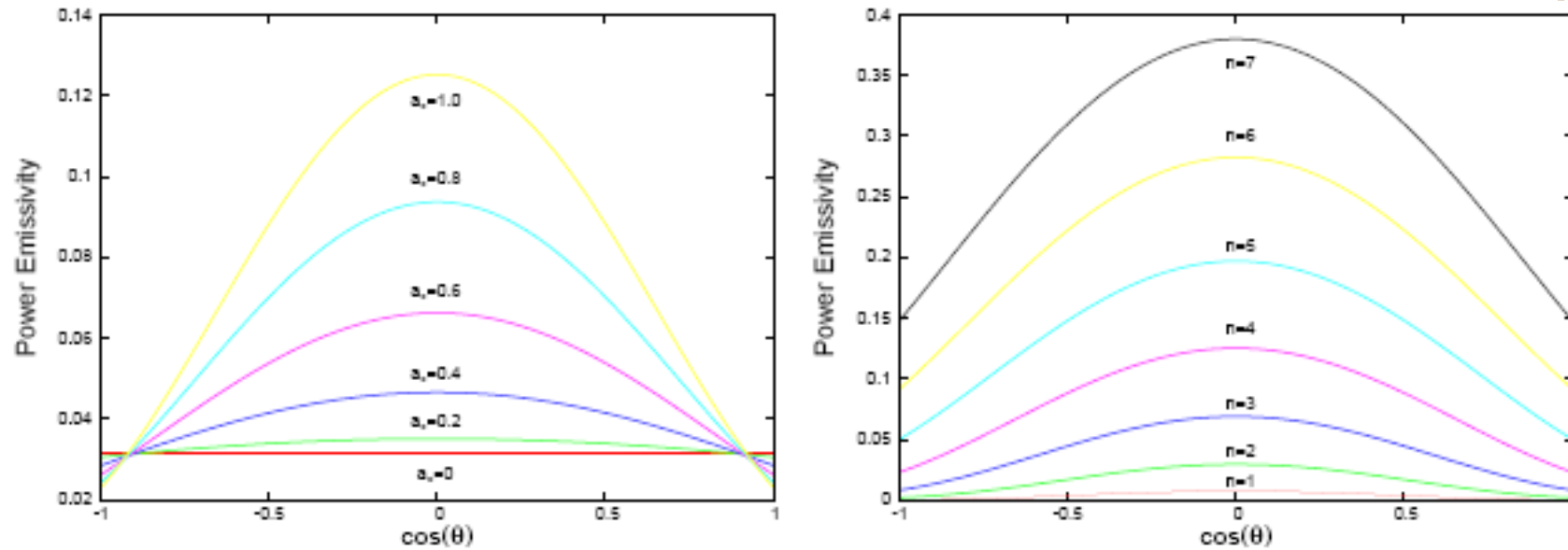
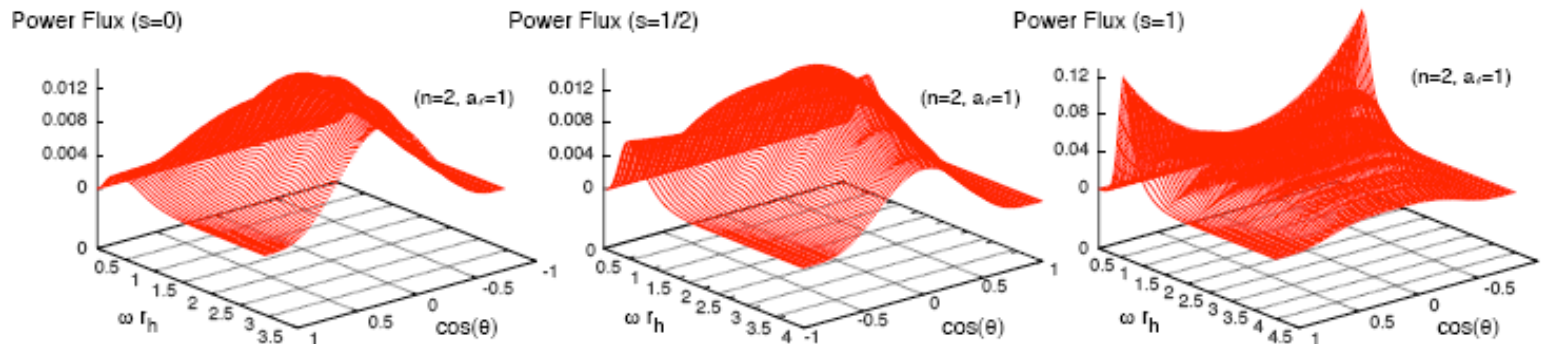


Figure 13: Power emissivity for scalar emission on the brane from a rotating black hole as a function of $\cos \theta$, (a) for $n = 4$ and variable a_* , and (b) for $a_* = 1$ and variable n .



Spin comparisons

- Equatorial (centrifugal) bulge
- Strong polar (& polarized) emission of vectors

All analyses strongly indicate that BH decay is brane dominated partly due to the very large number of SM degrees of freedom

| Particle | Scalar | Spinor | Vector |
|----------|--------|--------|--------|
| Quark | | 72 | |
| Gluon | | | 16 |
| Lepton | | 12 | |
| Neutrino | | 6* | |
| Photon | | | 2 |
| Z | 1 | | 2 |
| W | 2 | | 4 |
| Higgs | 1 | | |
| Total | 4 | 90 | 24 |

For the non-rotating Schwarzschild case these results are definitive:

Cardoso etal.
Kanti etal.

TABLE IV: Percentage of power going into each field species for the minimal $U(1) \times SU(2) \times SU(3)$ standard model with three families and one Higgs field above the spontaneous symmetry breaking scale. The four-dimensional results are taken from Ref. [15] and the higher dimensional results for fermions and gauge fields are taken from Ref. [9].

| D | 4 | 5 | 6 | 7 | 8 | 9 | 10 | 11 |
|--------------|------|------|------|------|------|------|------|------|
| Scalars | 6.8 | 4.0 | 3.7 | 3.6 | 3.6 | 3.5 | 3.3 | 2.9 |
| Fermions | 83.8 | 78.7 | 75.0 | 72.3 | 69.9 | 66.6 | 61.6 | 53.4 |
| Gauge Bosons | 9.3 | 16.7 | 20.0 | 21.7 | 22.3 | 22.2 | 20.7 | 18.6 |
| Gravitons | 0.1 | 0.6 | 1.3 | 2.4 | 4.2 | 7.7 | 14.4 | 25.1 |

For the rotating case the GBF calculations are incomplete but the expectation is that this result is robust at least at the semi-quantitative level. Evidence for this can clearly be seen in the ‘rotating’ scalar case :

26

Panagiota Kanti

Table 7 Bulk-to-Brane Relative Emissivities Ratio for scalar fields in terms of n

| | $n = 0$ | $n = 1$ | $n = 2$ | $n = 3$ | $n = 4$ | $n = 5$ | $n = 6$ | $n = 7$ |
|------------|---------|---------|---------|---------|---------|---------|---------|---------|
| Bulk/Brane | 1.0 | 0.40 | 0.24 | 0.22 | 0.24 | 0.33 | 0.52 | 0.93 |

35

Finite BH mass, 'cooling' and the remnant possibility can be corrected for in the original energy distribution by making the replacement (canonical-> microcanonical description)

$$\int_0^{\infty} d\omega \frac{\omega^3}{e^{\omega/T} + s_i} \longrightarrow \int_{m_{\text{crit}}}^m dy (m - y)^{d+3} \left[e^{S(m)-S(y)} + s_i \right]^{-1}$$

Here $d=0$ for brane emission, S is the BH entropy as a function of the BH mass, and m_{crit} is a lower bound on the BH mass if a remnant occurs in the model of interest. Note $S(m)-S(y) \rightarrow (m-y)/T + \dots \rightarrow \omega/T$ in the limit that the mass does not change during particle emission and we recover the usual expression.

This can be a sizeable correction as the BH is not an infinite sink and the energies of the emitted states are not so much smaller than the BH mass itself.

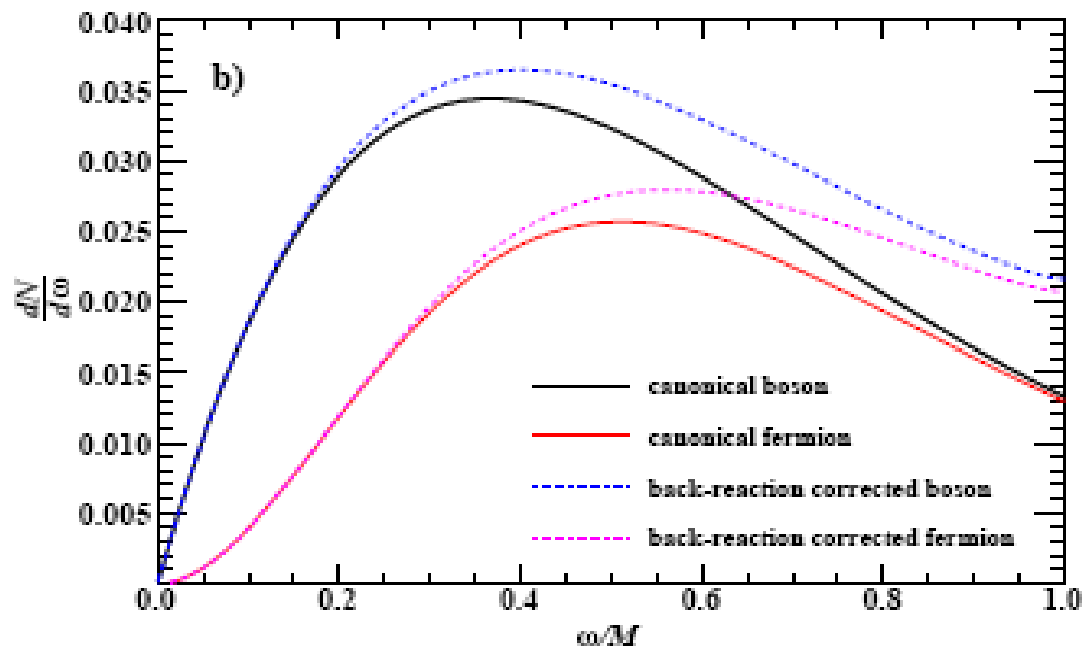
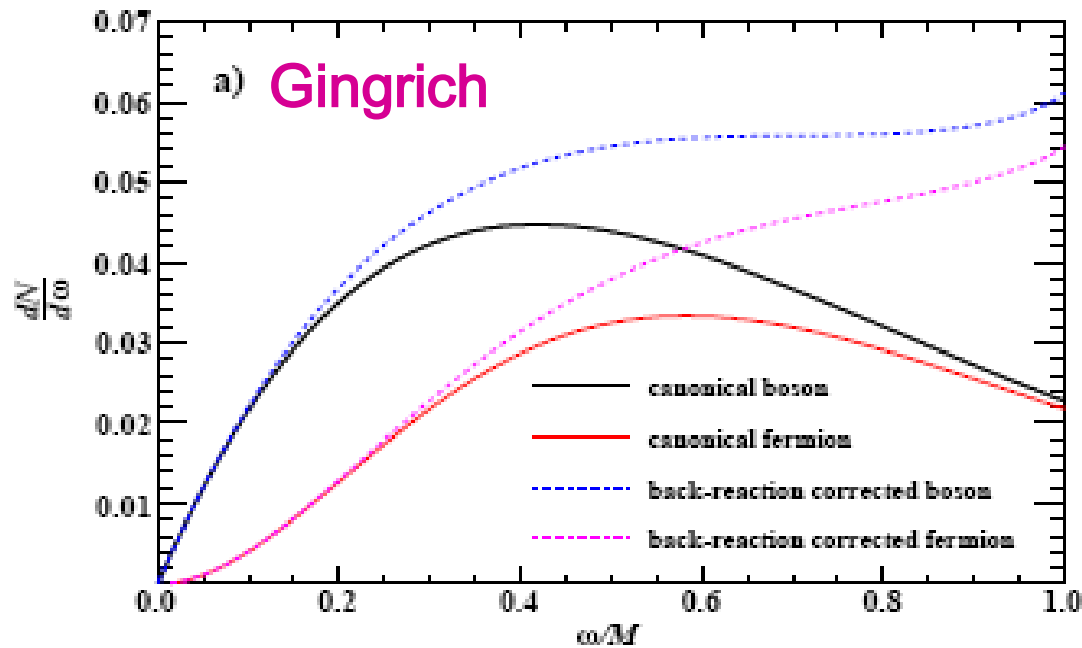
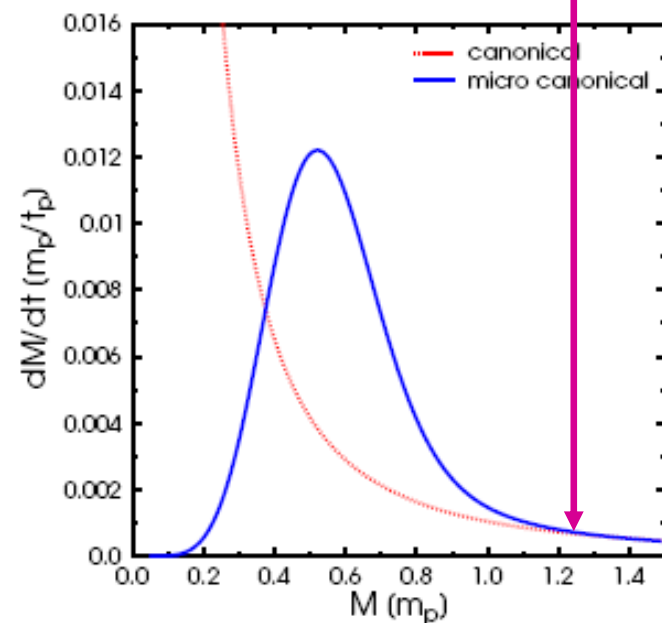


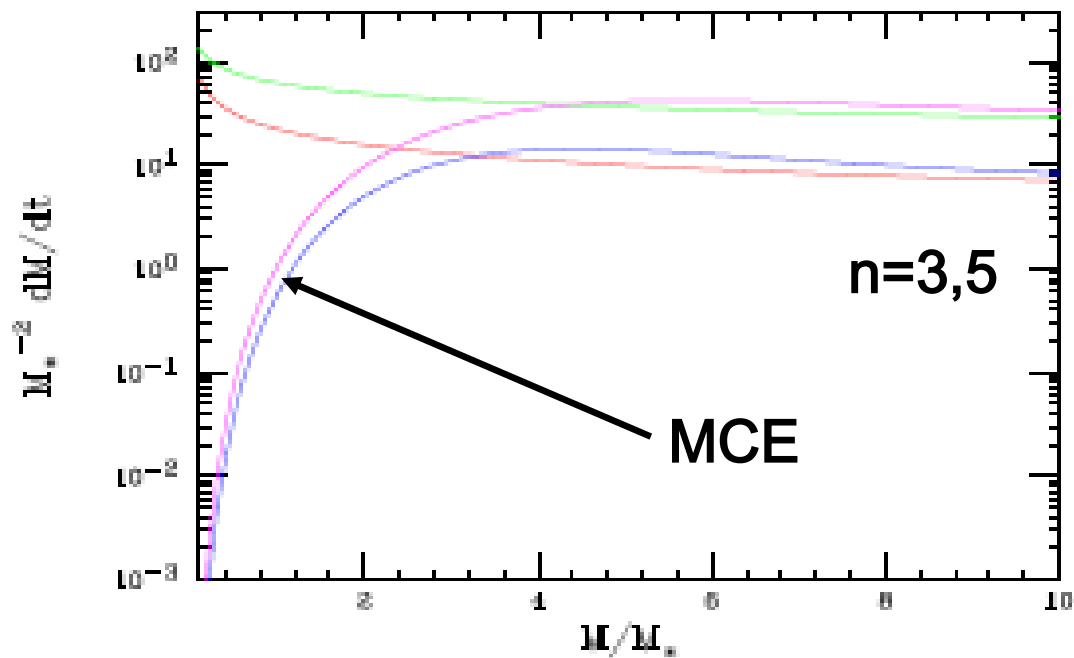
Figure 1. Energy spectra for $M = M_P = 1$ TeV. a) $n = 2$, $T = 260$ GeV, $S = 4$
 b) $n = 7$, $T = 230$ GeV, $S = 4$.

Note the enhancement at high ω values which leads to, e.g., a change in the BH lifetime..

The two treatments will coincide when $M_{BH} \gg M_*$ so that 'cooling' can be neglected.

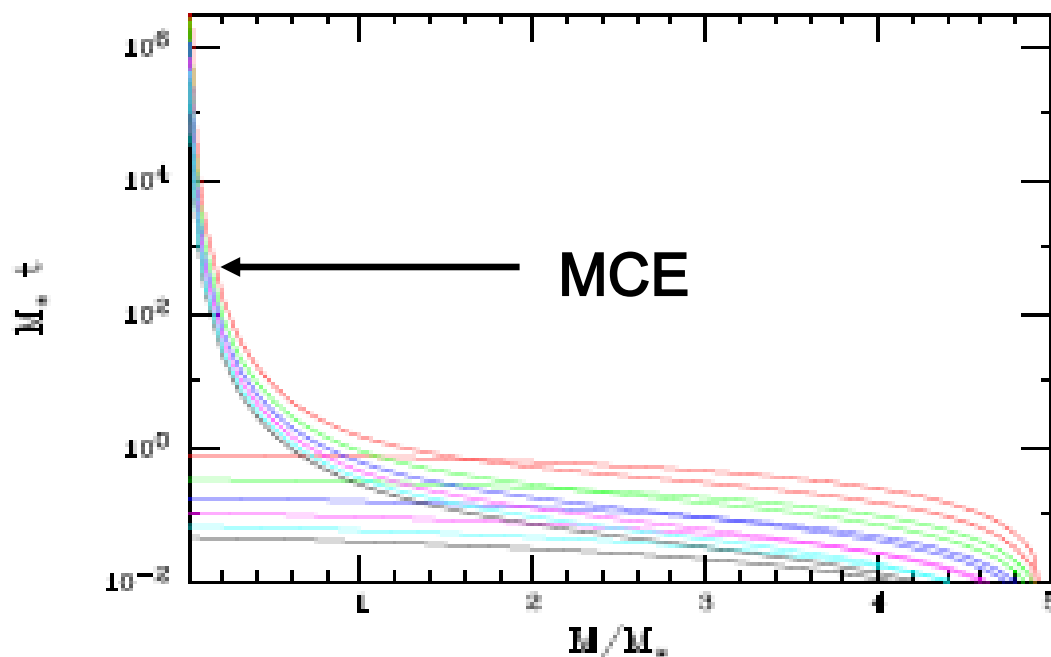


Hossenfelder



The BH is not an infinite heat source..

Note that BH lifetimes become significantly longer in the MCE treatment and would be more resonance-like



hep-ph/0601028

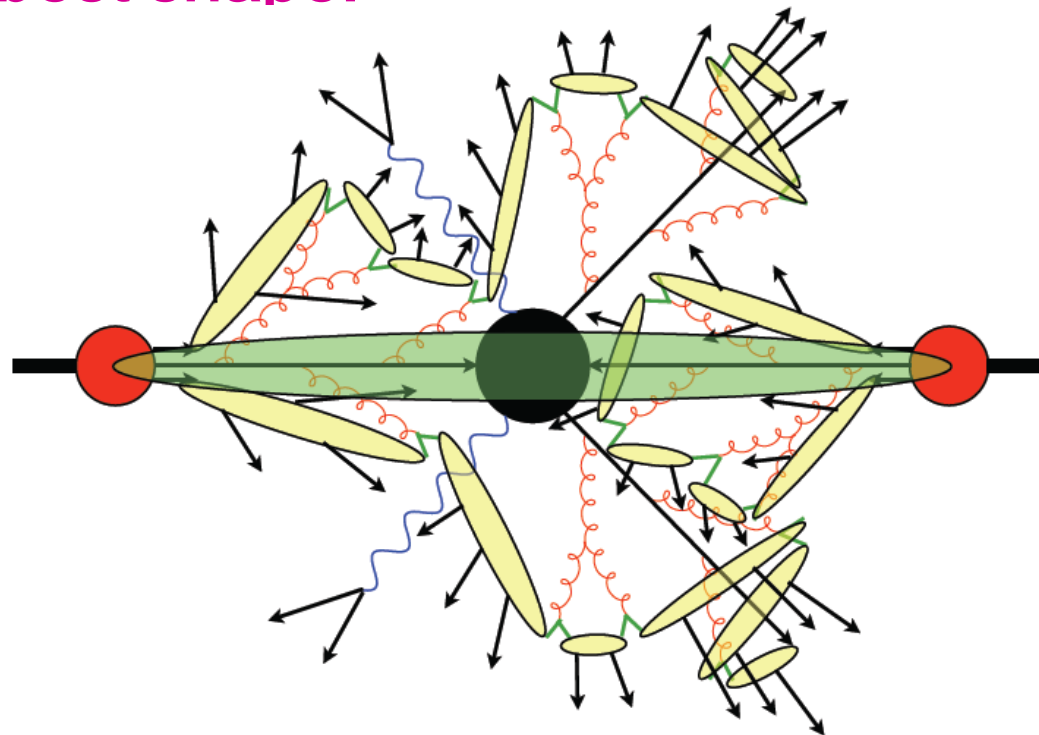
Figure 4: (Top) Rate of change of the BH mass through Hawking radiation on the brane assuming the EH action as discussed in the text; the CE(top) and MCE(bottom) results are represented by the two sets of curves with the case $n = 5(3)$ being the upper(lower) curve. (Bottom) Decay times for a BH with an initial $m = M_{BH}/M_p = 5$; the rising(flat) set of curves at low m corresponds to the MCE(CE) case. In each set of curves n ranges from 2 to 7 going from top to bottom.

BH leaving our brane by graviton recoil...

...I think I'll leave this for another talk....

So what do BH look like at the LHC?

- As you may have guessed **none** of the available Monte Carlos for BH production & decay at colliders contain all (or even most) of the various aspects discussed above...but they are still in an **evolving state**.
- As usual, the MCs lag the theoretical developments by some interval and one must remember that even the 'theory side' is **not yet** in the best shape.



Black Hole Event Generators

- **TRUENOIR** (Dimopoulos & Landsberg, hep-ph/0106295)
 - ➔ $J=0$ only; no energy loss; fixed T ; no g.b.f.
 - **CHARYBDIS** (Harris, Richardson & BW, hep-ph/0307305)
 - ➔ $J=0$ only; no energy loss; variable T ; g.b.f. included
 - **CATFISH** (Cavaglia et al., hep-ph/0609001)
 - ➔ $J=0$ only; energy loss option; variable T ; g.b.f. included
 - **BlackMax** (Dai et al., arXiv:0711.3012)
 - ➔ $J \neq 0$; energy loss option; variable T ; split branes; g.b.f.
 - **CHARYBDIS2** (Casals et al., ~~in preparation~~) **just released**
 - ➔ $J \neq 0$; energy loss model; variable T ; remnant options; g.b.f.
- ➔ All need interfacing to a parton shower and hadronization generator (PYTHIA or HERWIG)

| D | 4 | 5 | 6 | 7 | 8 | 9 | 10 | 11 | BB |
|-----------------|------|------|------|------|------|------|------|------|------|
| quarks | 0.71 | 0.66 | 0.62 | 0.59 | 0.57 | 0.55 | 0.53 | 0.51 | 0.56 |
| charged leptons | 0.12 | 0.11 | 0.10 | 0.10 | 0.10 | 0.09 | 0.09 | 0.09 | 0.09 |
| neutrinos | 0.06 | 0.06 | 0.05 | 0.05 | 0.05 | 0.05 | 0.04 | 0.04 | 0.05 |
| gluons | 0.05 | 0.09 | 0.12 | 0.14 | 0.15 | 0.16 | 0.16 | 0.16 | 0.17 |
| photon | 0.01 | 0.01 | 0.02 | 0.02 | 0.02 | 0.02 | 0.02 | 0.02 | 0.02 |
| EW bosons | 0.03 | 0.05 | 0.07 | 0.08 | 0.09 | 0.09 | 0.09 | 0.09 | 0.09 |
| Higgs | 0.03 | 0.01 | 0.01 | 0.01 | 0.01 | 0.01 | 0.01 | 0.01 | 0.01 |
| graviton | 0.00 | 0.00 | 0.01 | 0.01 | 0.02 | 0.03 | 0.05 | 0.08 | 0.01 |

Table 3: Probability of emission for different particles.

BH are most likely to decay to multi-jet final states along w/ leptons, neutrinos (MET) and gauge bosons

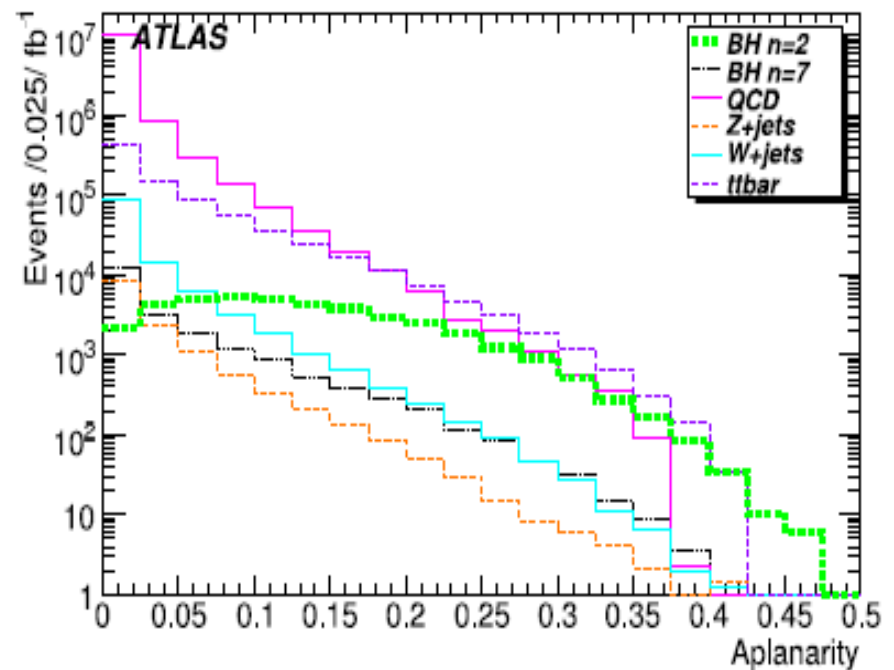
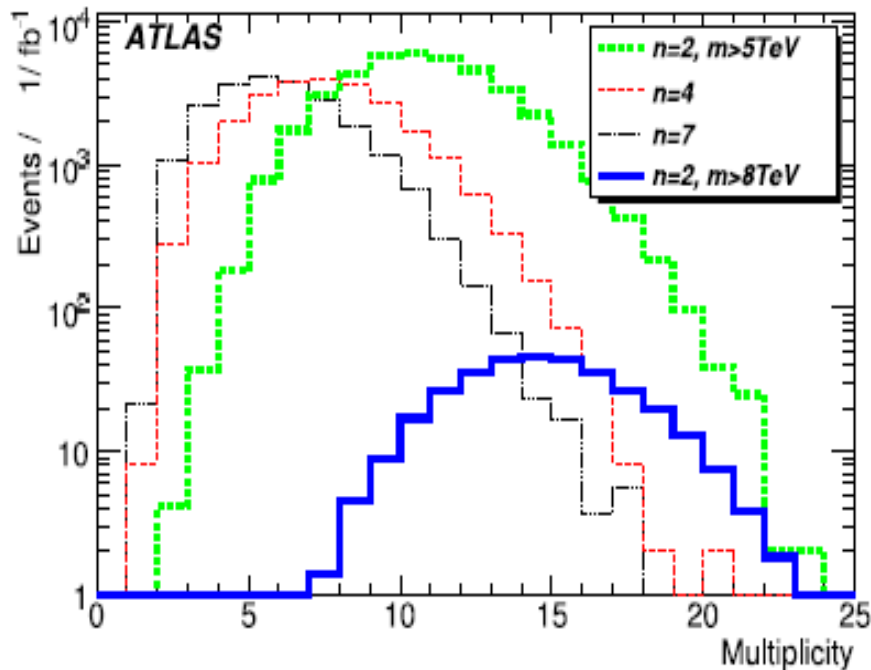


Figure 1. (left) Multiplicity of reconstructed objects for four black hole samples: three samples with black hole masses $M_{\text{BH}} > 5 \text{ TeV}$ and with $n = 2$ (black), 4 (red) and 7 (green) extra dimensions, as well as one sample with $n = 2$ and $M_{\text{BH}} > 8 \text{ TeV}$. All samples are simulated with the gravity scale of $M_D = 1 \text{ TeV}$; (right) Event aplanarity for two black hole samples with $M_{\text{BH}} > 5 \text{ TeV}$ and $n = 2$ (green) and $n = 7$ (black), as well as for QCD dijet (magenta), $t\bar{t}$ (violet), $Z + \text{jet}$ (orange) and $W + \text{jet}$ (cyan) backgrounds.

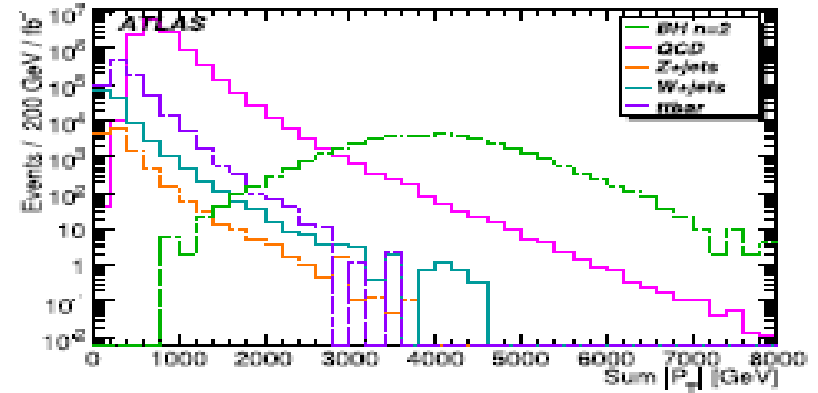
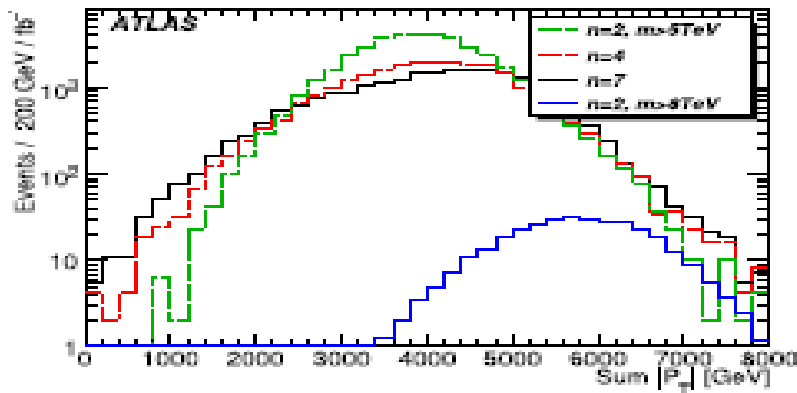


Figure 3. $\sum |p_T|$ distributions for (left) black hole samples and (right) backgrounds (QCD dijet, $t\bar{t}$ and $W/Z + \text{jet}$), along with one signal sample for reference.

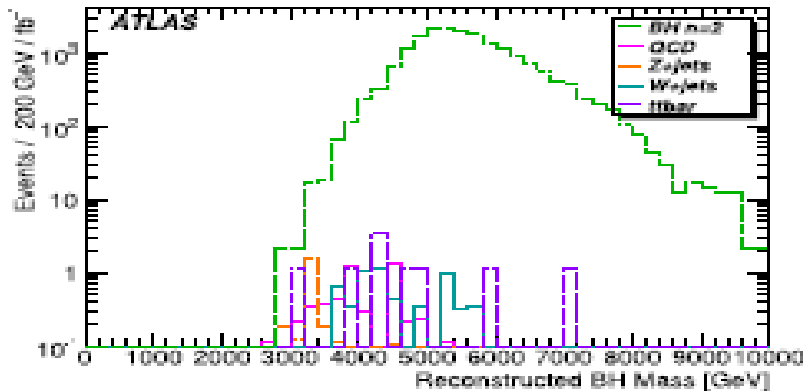


Figure 4. Black hole mass distribution with requirements $\sum |p_T| > 2.5 \text{ TeV}$ and lepton $p_T > 50 \text{ GeV}$ for the signal sample with $n = 2$ and $M_{\text{BH}} > 5 \text{ TeV}$, and for backgrounds.

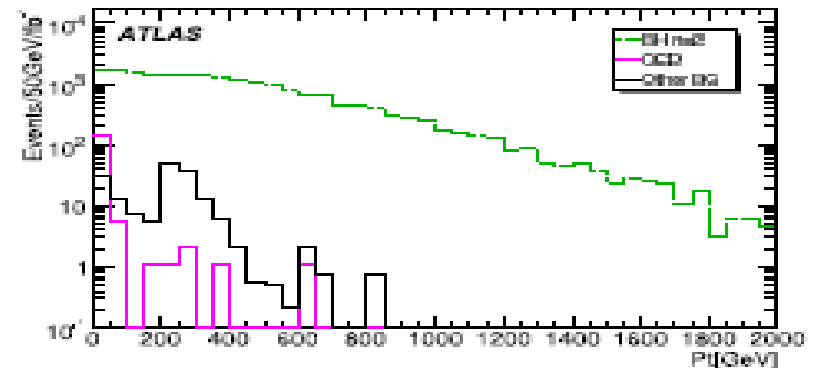
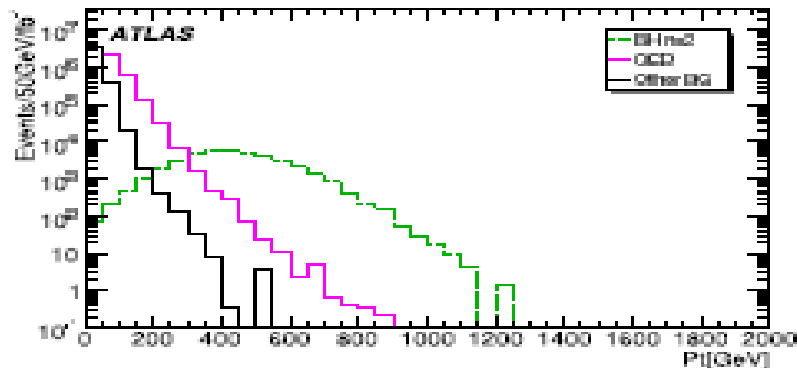


Figure 5. Event selection variables for the black hole sample with $n = 2$ and $M_{\text{BH}} > 5 \text{ TeV}$ and for backgrounds: (left) p_T distribution of 4th-leading object out of all selected objects; (right) p_T distribution of the leading lepton (electron or muon) after requiring at least four reconstructed objects with $p_T > 200 \text{ GeV}$.

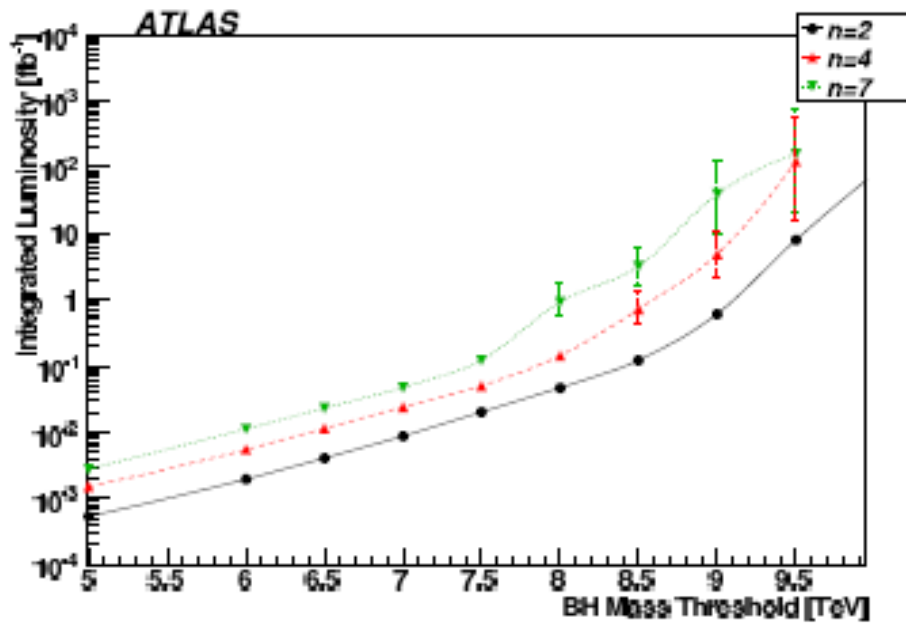


Figure 6. Discovery potential using $\sum |p_T|$ and lepton cuts: Required luminosity as a function of black hole mass production threshold for scenarios with $M_D = 1$ TeV and $n = 2$ (black), 4 (red) and 7 (green) extra dimensions.

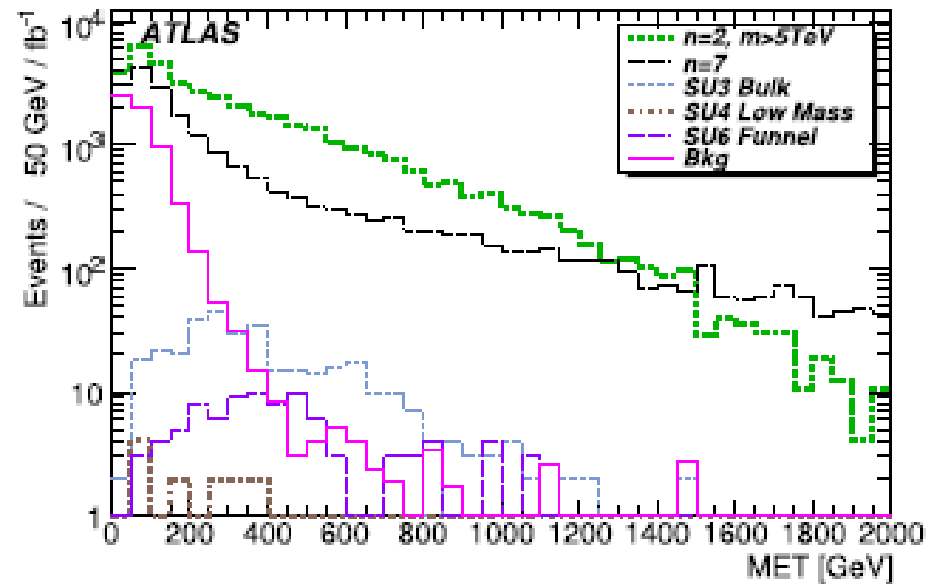
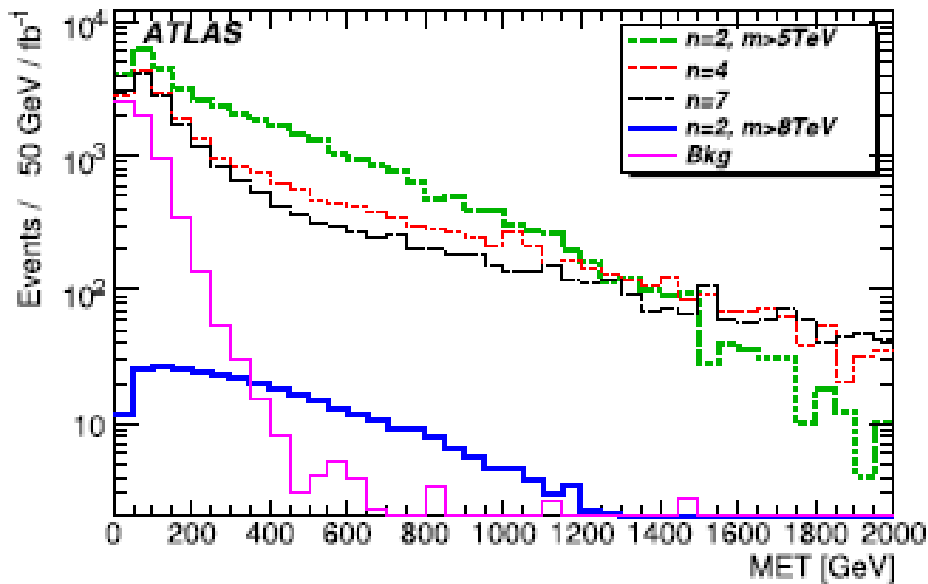


Figure 7. Missing transverse energy after the $\sum |p_T| > 2.5$ TeV cut: (left) E_T^{miss} for different black hole event samples and for the sum of simulated SM backgrounds; (right) E_T^{miss} for two black hole samples contrasted with three Supersymmetric models with a range of mass scales.

Black Holes – Generator Studies

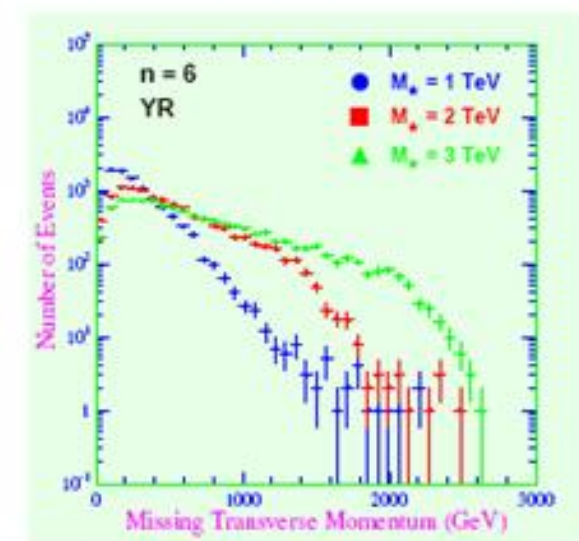
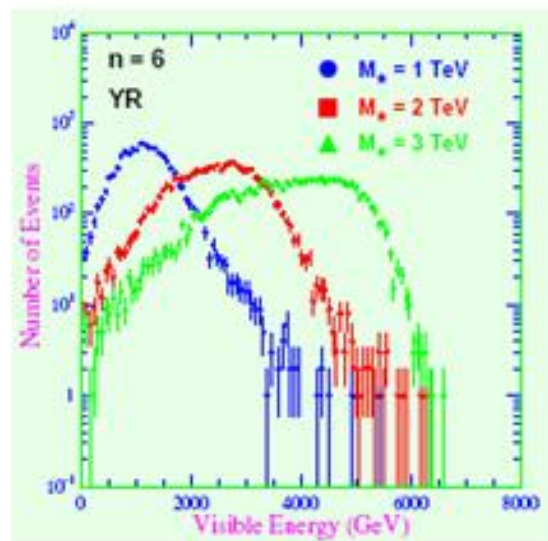
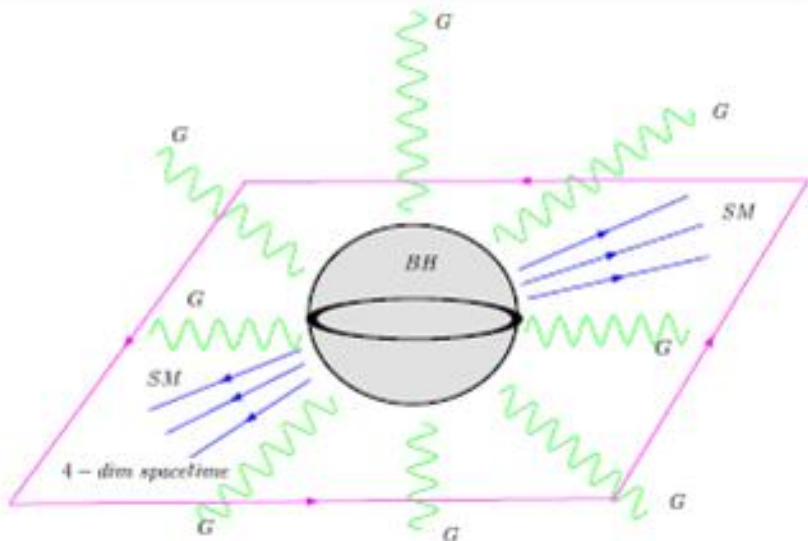
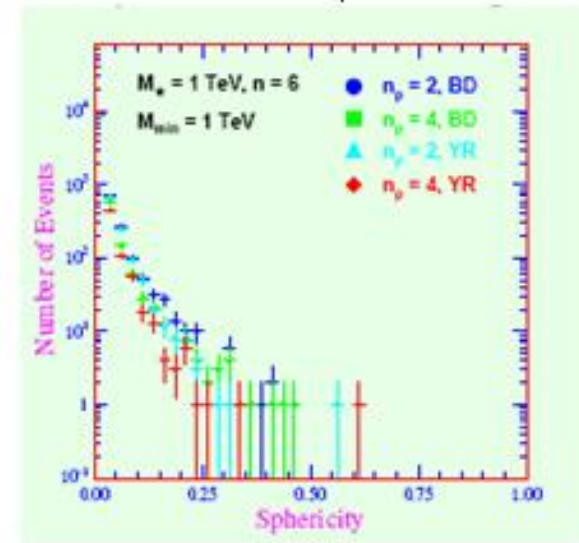
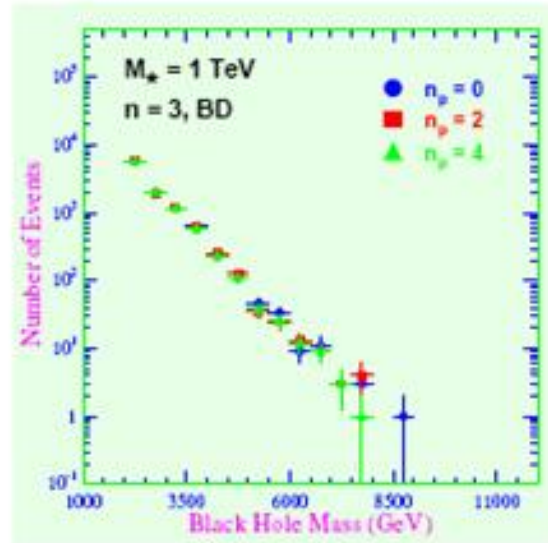


CATFISH authors: M. Cavaglià, R. Godang, L. Cremaldi, D. Summers

CATFISH

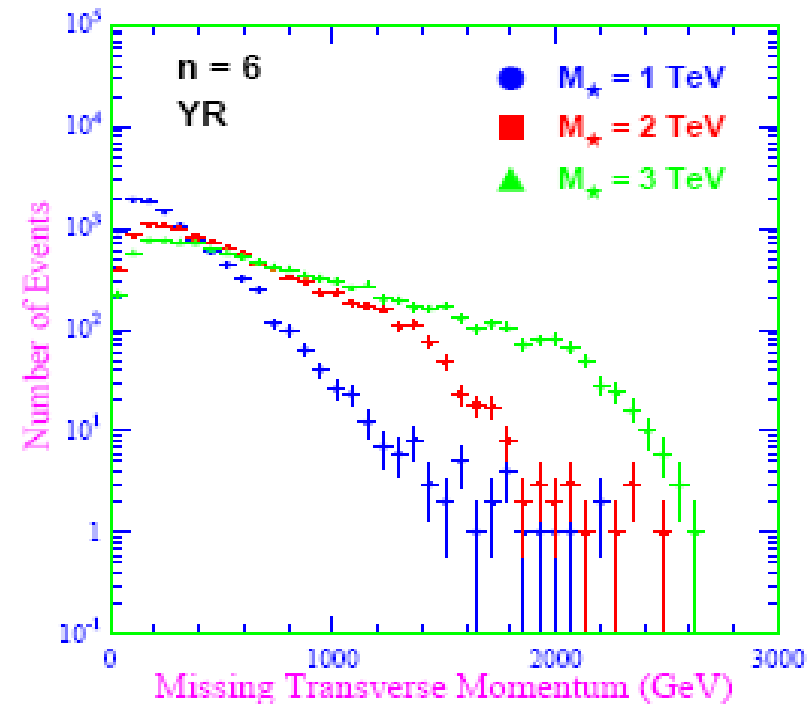
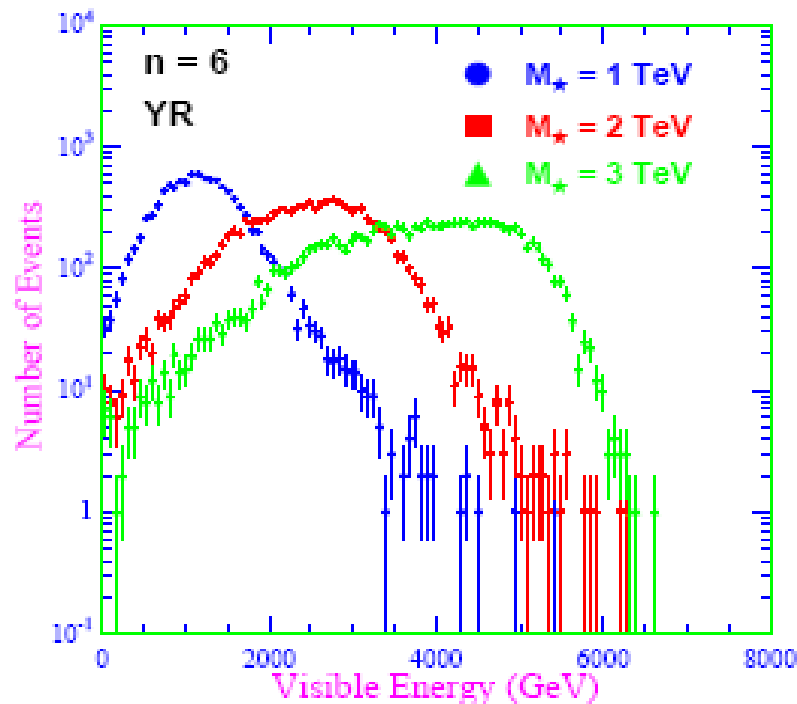
- Collider grAviTational Field Simulator for black Holes

Comput.Phys.Commun. 177:506-517, 2007



Effects of Fundamental Scale

- Visible energy and missing transverse momentum for $n = 6$, $n_p = 4$, YR



- Increasing M_* leads to higher M_{min} ($M_{min} = 2M_*$) :

- Larger visible energy in Hawking phase
- Larger missing transverse momentum

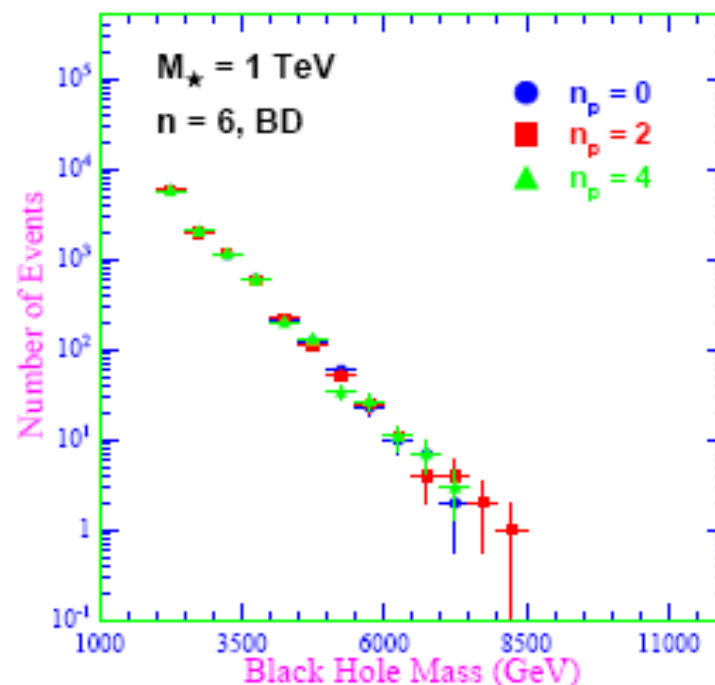
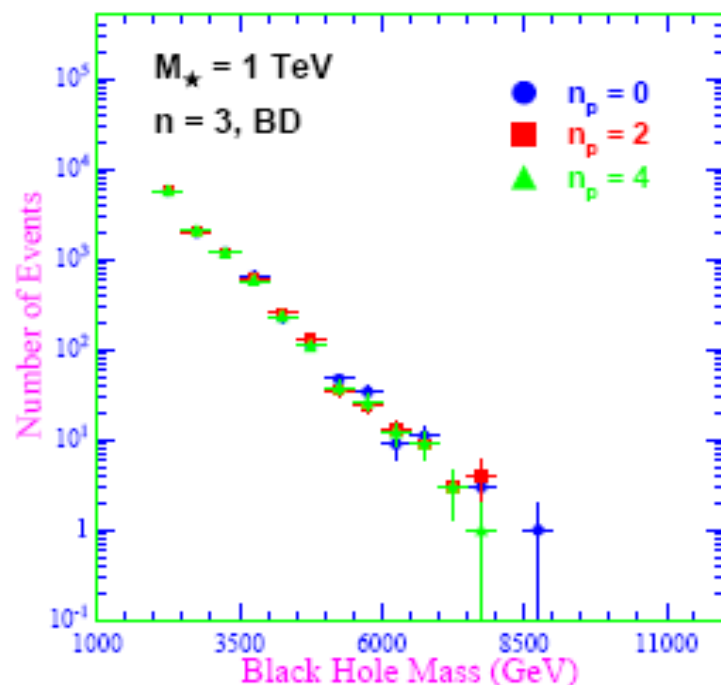
CMS

- If BHs are observed at LHC $\implies M_*$ could be measured to a certain degree of precision

Effects of Final BH Decay

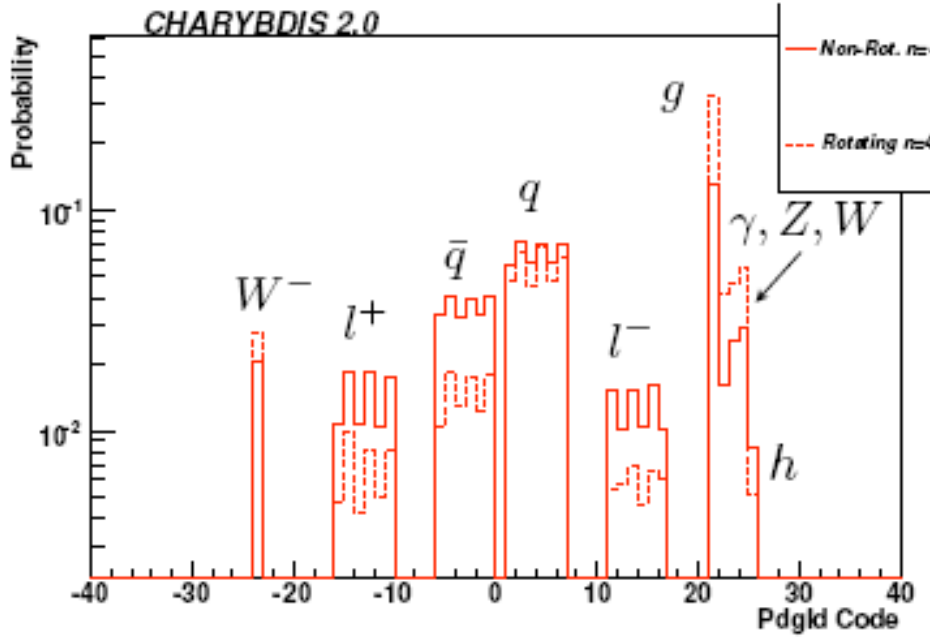
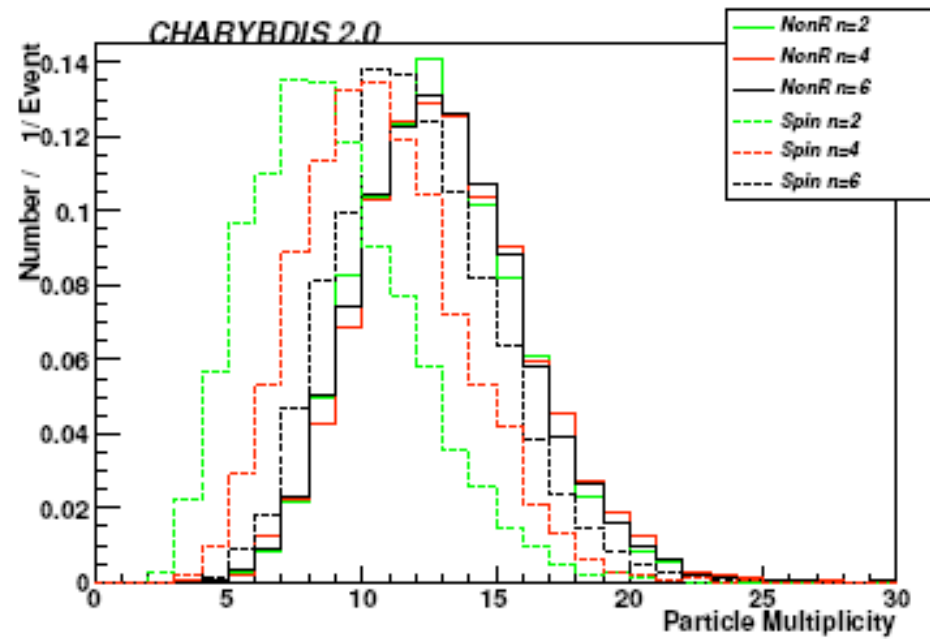
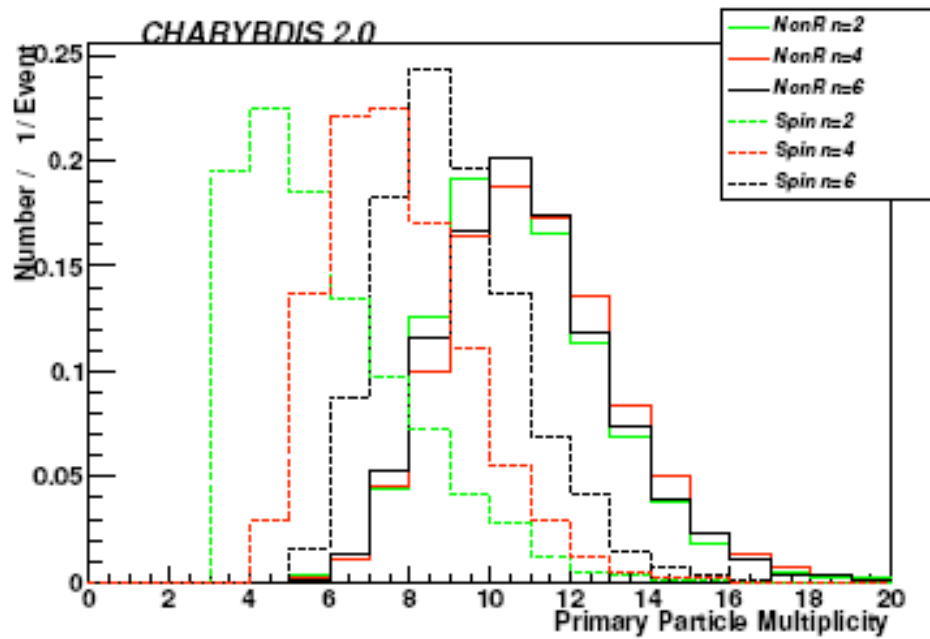
CMS

- BH Mass distribution for $M_{\star} = 1$ TeV, ($n = 3, 6$), BD



- The initial BH mass is obviously unaffected by the detail of final decay
 - (left) We vary number of quanta at the end of BH decay for $n = 3$
 - (right) We vary number of quanta at the end of BH decay for $n = 6$
- This is a nice consistency check of CATFISH code

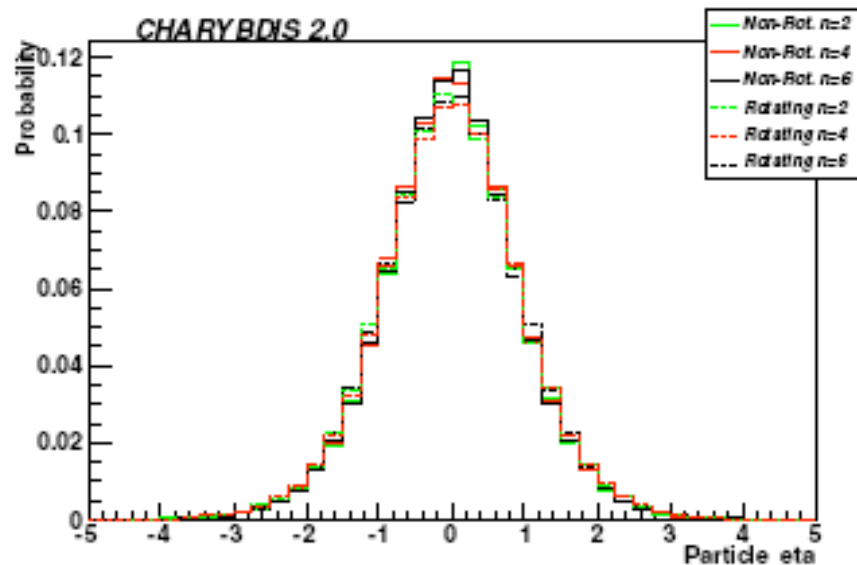
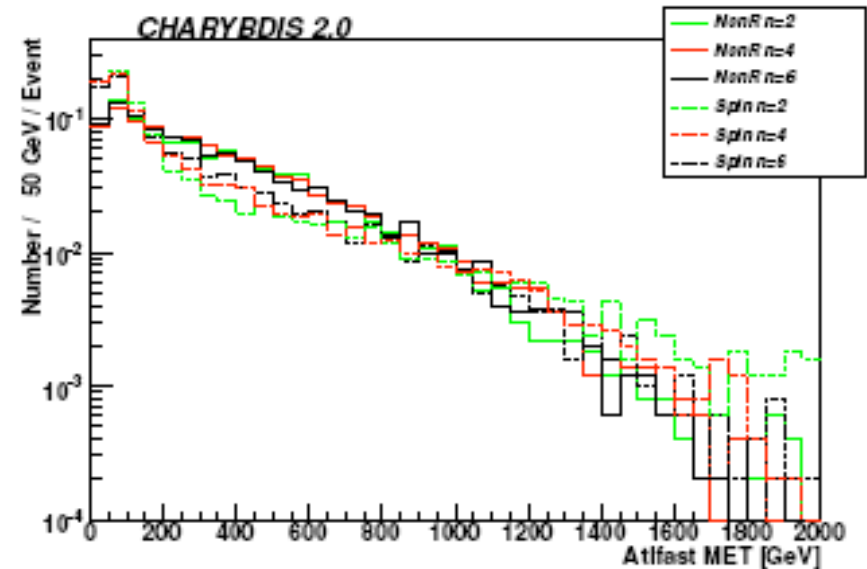
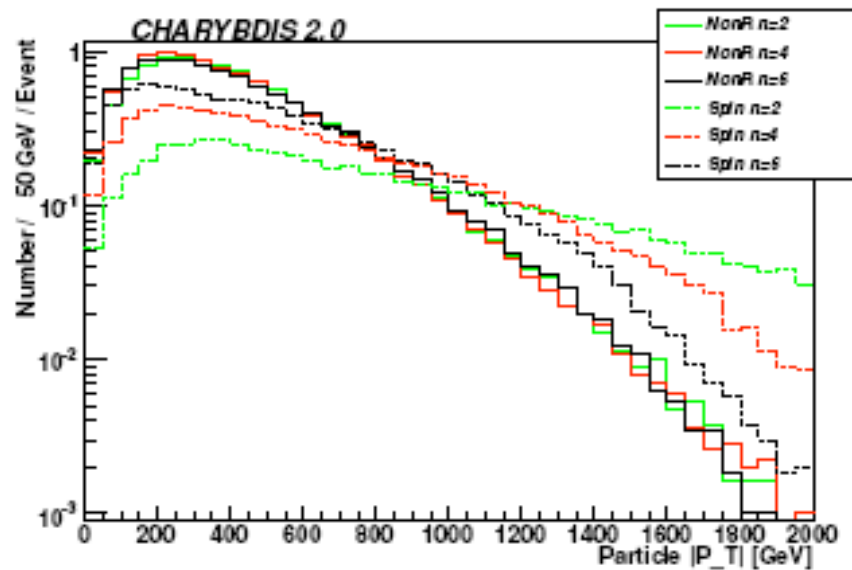
Observable effects of BH spin?



- Higher power flux
- ➔ Fewer, more energetic particles
- Enhanced vector emission
- ➔ More gluons, photons, W, Z
- ➔ Aligned with BH axis, polarized

B. Webber

Effects of BH Spin (2)



- Harder spectrum & MET
- Oblate distribution
- ➔ (Slightly) higher rapidities

B. Webber

Summary

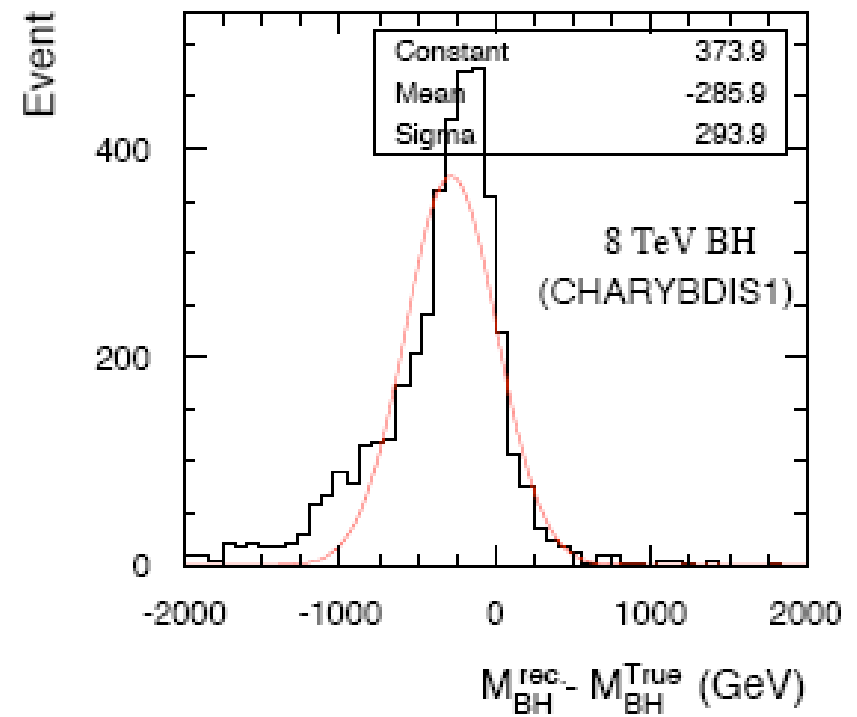
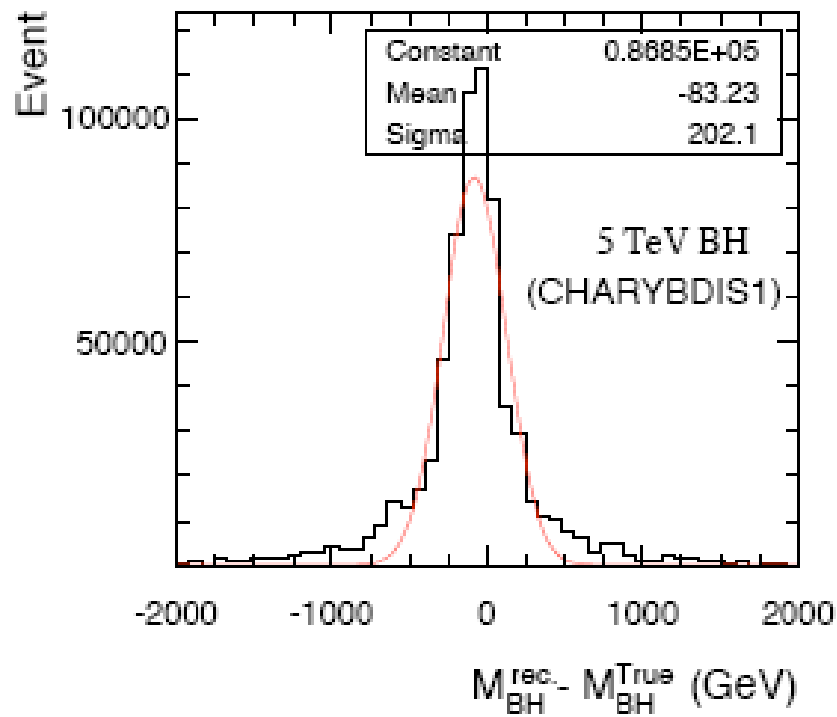
- A real picture of TeV scale BH is hampered by not having a fully-calculable theory of quantum gravity but much progress has still been made since 2001.
- TeV BH physics is based on GR + semi-quantum phenomena and a lot of 'toy model' concepts which capture various possible 'quantum' aspects of BH physics. No complete picture exists.
- A hope (dream) is that TeV BH *ARE* seen at the LHC so that we can learn about this physics from actual *DATA* so that we can construct such a theory.
- Current MC lag the theoretical developments but Charybdis2 certainly has the most flexibility and features
- **Exciting times lie ahead at the LHC**

BACK-UP SLIDES

Table 1: Default CHARYBDIS2 generator parameters.

| Name | Description | Default |
|--------------|--|---------|
| MINMSS | Minimum parton-parton invariant mass | 5 TeV |
| MAXMSS | Maximum parton-parton invariant mass | 14 TeV |
| MPLNCK | Planck scale | 1 TeV |
| MSSDEF | Convention for Planck scale | 3 |
| TOTDIM | Total number of dimensions | 6 |
| NBODY | Number of particles in remnant decay | 2 |
| TIMVAR | Allow T_H to evolve with BH parameters | .TRUE. |
| MSSDEC | Allowed decay products (3=all SM) | 3 |
| GRYBDY | Include grey-body effects | .TRUE. |
| KINCUT | Use a kinematic cut-off on the decay | .FALSE. |
| THWMAX | Maximum Hawking temperature | 1 TeV |
| BHSPIN | Simulate rotating black holes | .TRUE. |
| BHJVAR | Allow black hole spin axis to vary | .TRUE. |
| MJLOST | Simulation of m , J lost in production/balding | .TRUE. |
| RMSTAB | Stable remnant model | .FALSE. |
| NBODYAVERAGE | Use flux criterion for remnant | .TRUE. |
| NBODYVAR | Variable-multiplicity remnant model | .FALSE. |
| NBODYPHASE | Use phase space for remnants | .FALSE. |
| SKIP2REMNANT | Bypass evaporation phase | .FALSE. |
| BOILING | Use boiling remnant model | .FALSE. |
| RMMINM | Minimum mass for boiling model | 100 GeV |

Measuring black hole masses



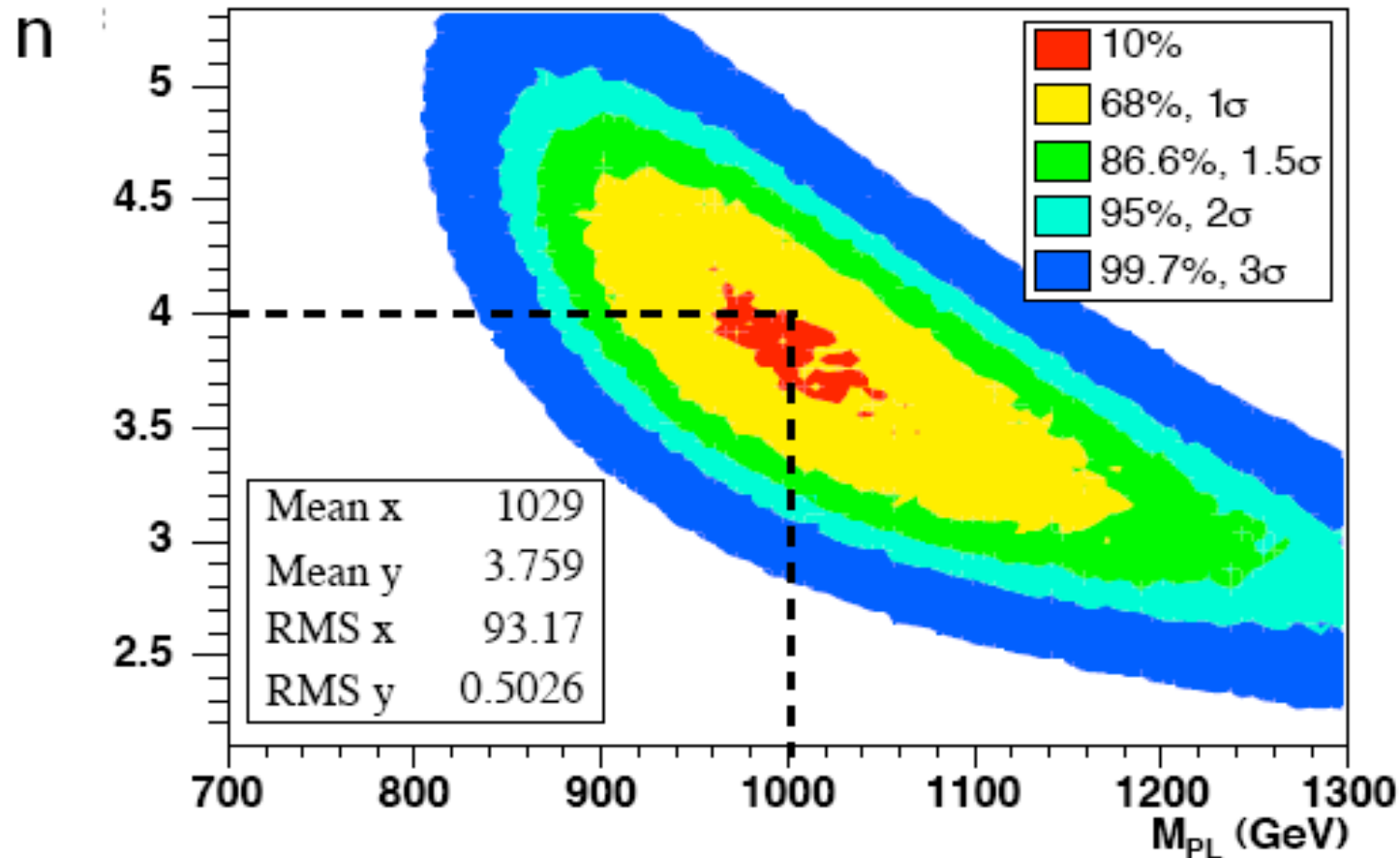
- Need $\cancel{E}_T < 100$ GeV for adequate resolution

→ $\Delta M_{\text{BH}} / M_{\text{BH}} \sim 4\%$

B. Webber

Combined measurement of M_{PL} and n

(CHARYBDIS1)



→ $\Delta M_{PL} / M_{PL} \sim 15\%$, $\Delta n \sim 0.75$ **B. Webber**

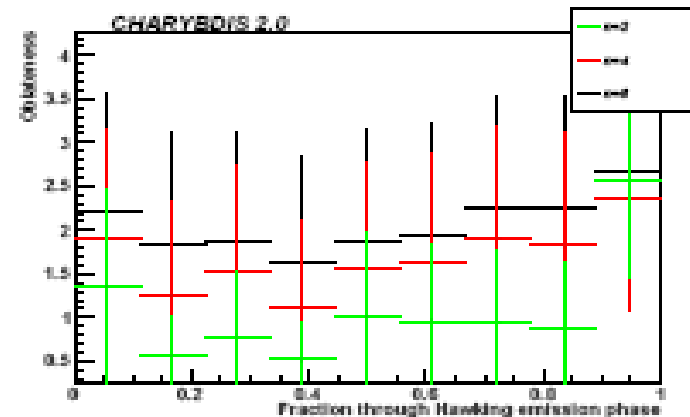
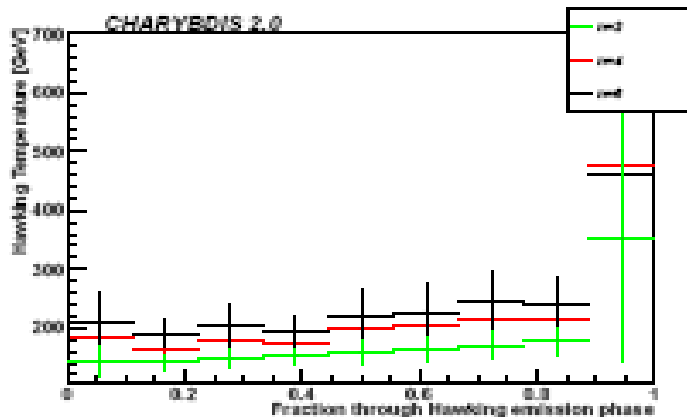
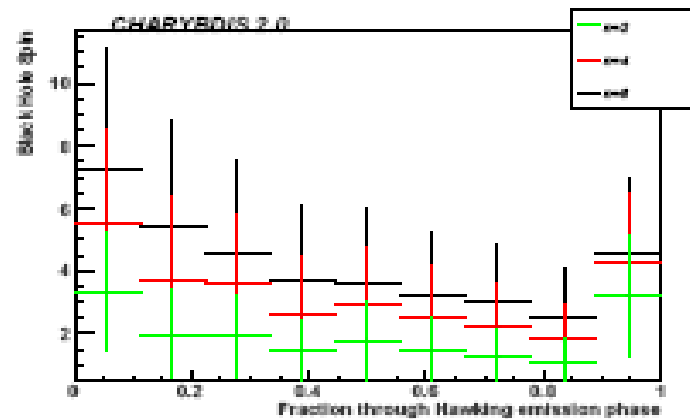
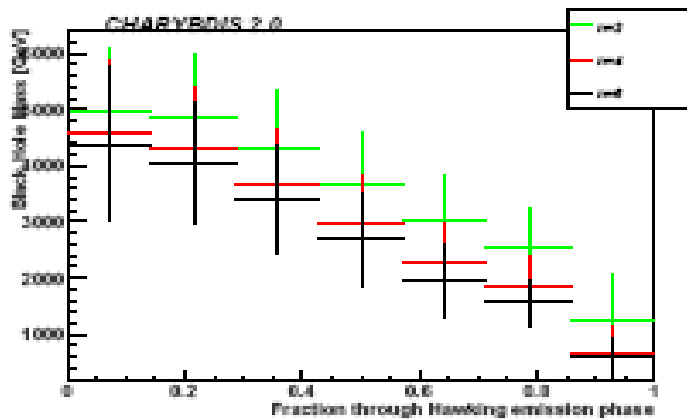
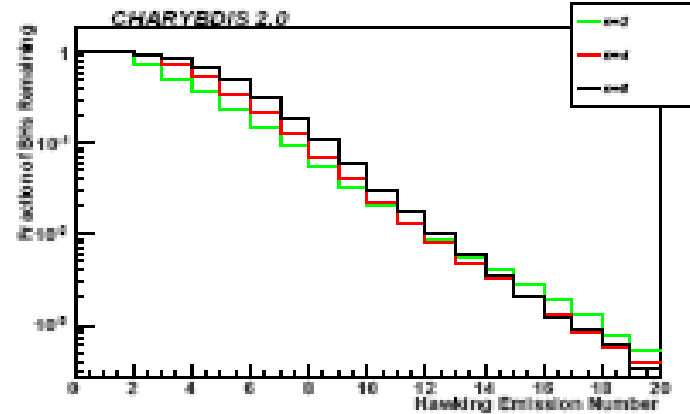
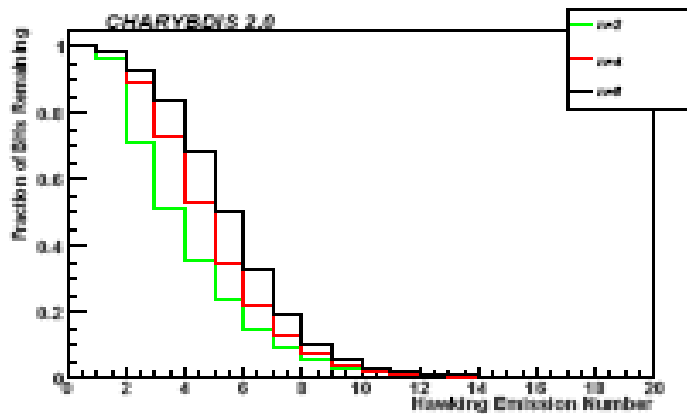


Figure 17: The evolution of black hole parameters during the Hawking evaporation phase. The lower two rows shows mean value of the relevant parameter after each emission, as a fraction of the total number of emissions in that event. Error bars indicate the standard deviation of the distribution.

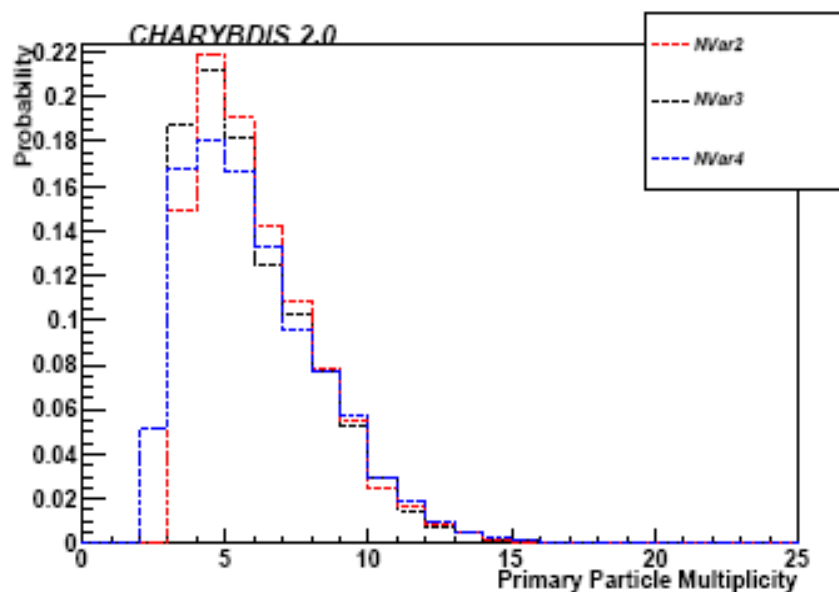
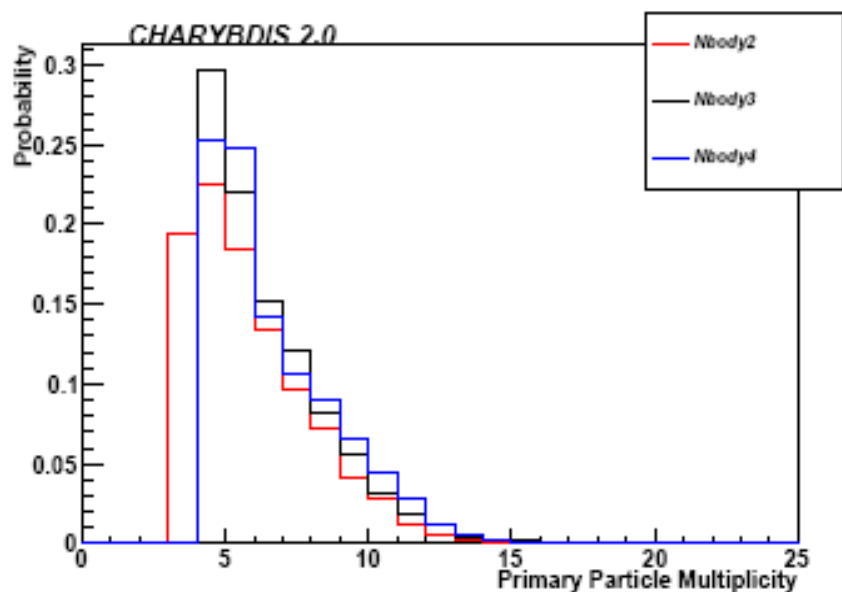
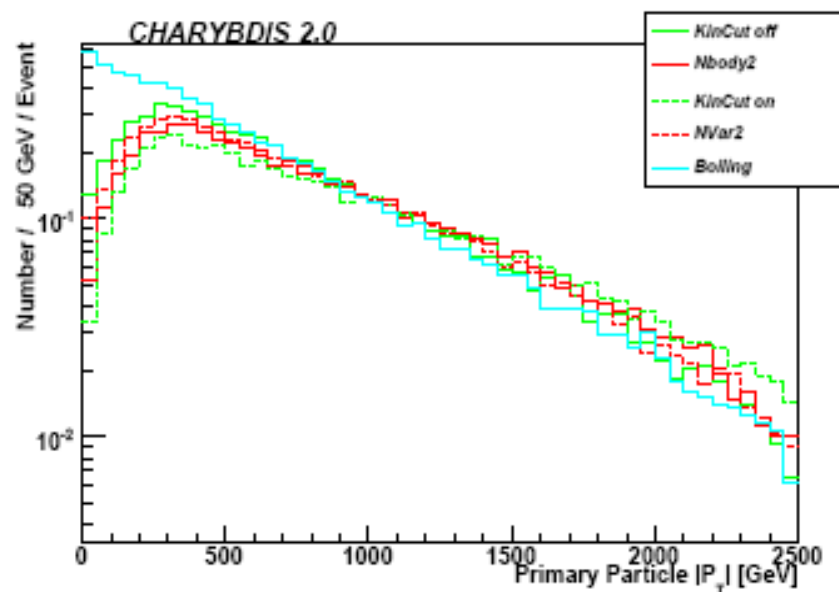
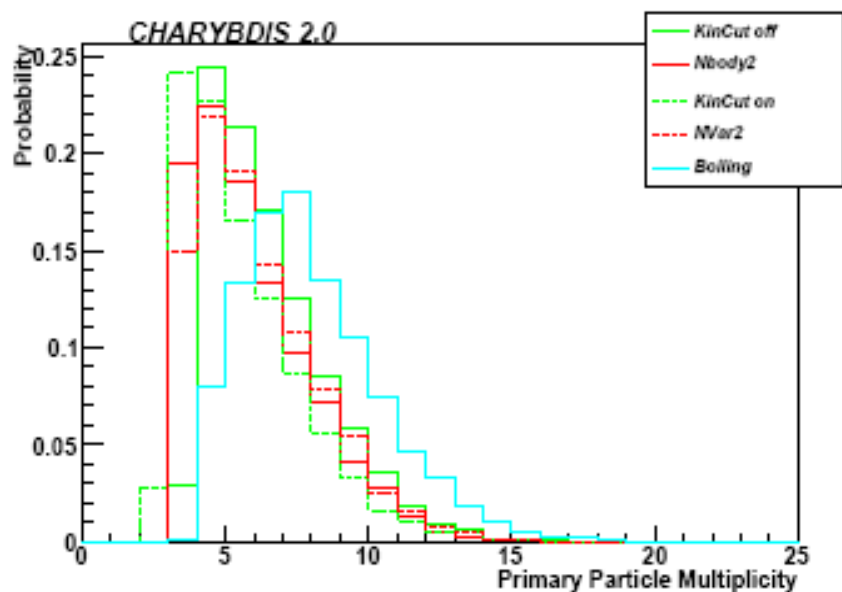


Figure 19: Primary particle distributions for black hole samples with $n=2$, using a wide range of remnant options, as defined in Table 2.

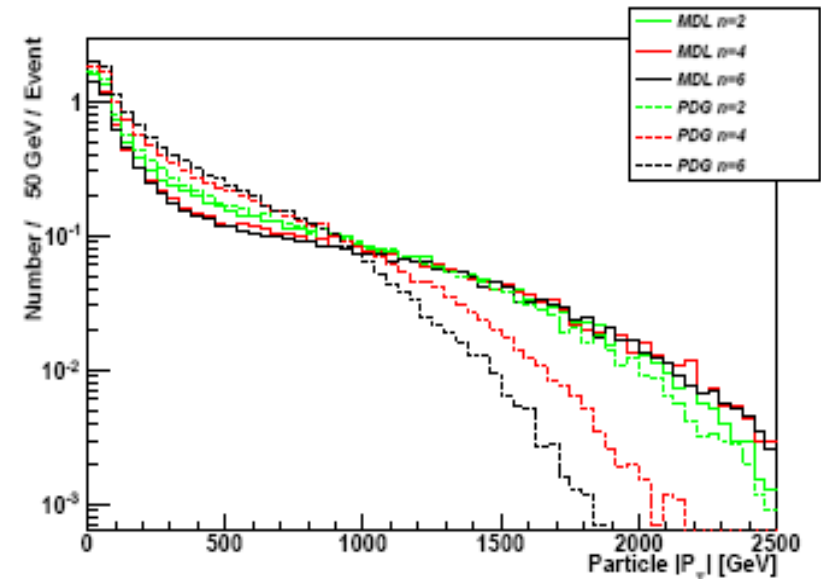
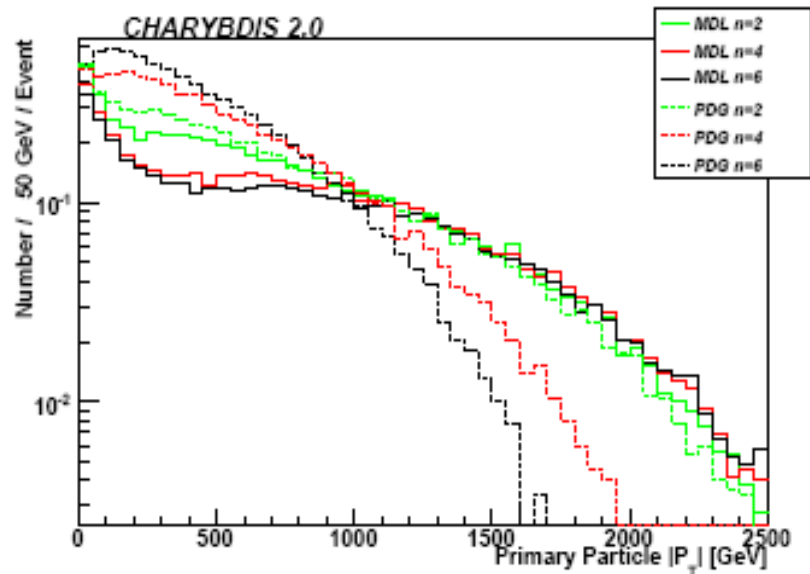
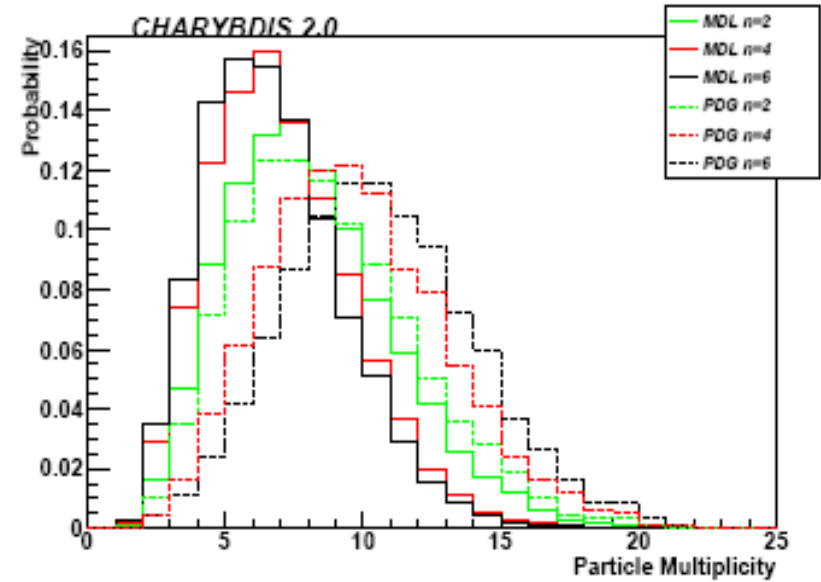
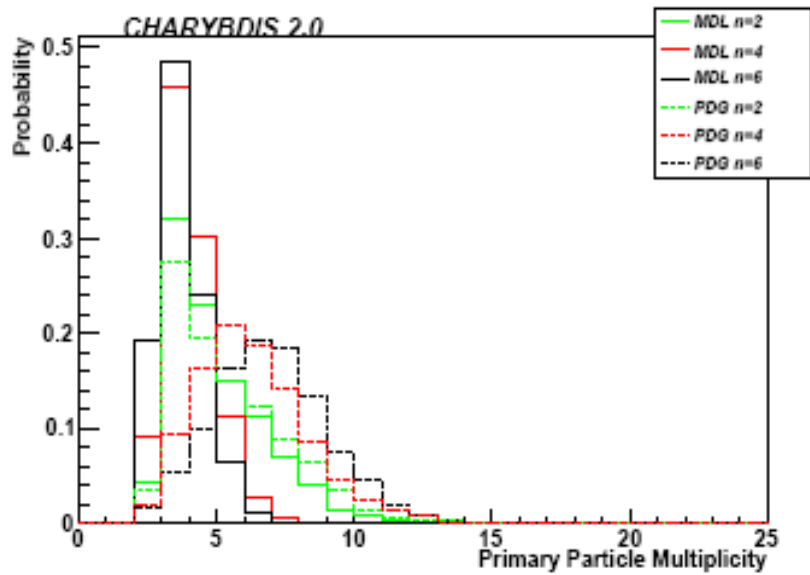


Figure 22: Particle Multiplicity distributions and P_T spectra at generator level (left) and after AcerDET detector simulation (right) for a 1 TeV Planck mass in PDG and Dimopoulos-Landsberg “MDL” conventions.